

Distributed Rate-Splitting Multiple Access for Multilayer Satellite Communications

Yunnuo Xu, Longfei Yin, *Student Member, IEEE*, Yijie Mao, *Member, IEEE*,
Wonjae Shin, *Senior Member, IEEE* and Bruno Clerckx, *Fellow, IEEE*

Abstract—Future wireless networks, in particular, 5G and beyond, are anticipated to deploy dense Low Earth Orbit (LEO) satellites to provide global coverage and broadband connectivity. However, the limited frequency band and the coexistence of multiple constellations bring new challenges for interference management. In this paper, we propose a robust multilayer interference management scheme for spectrum sharing in heterogeneous satellite networks with statistical channel state information (CSI) at the transmitter (CSIT) and receivers (CSIR). In the proposed scheme, Rate-Splitting Multiple Access (RSMA), as a general and powerful framework for interference management and multiple access strategies, is implemented distributedly at GEO and LEO satellites, coined Distributed-RSMA (D-RSMA). By doing so, D-RSMA aims to mitigate the interference and boost the user fairness of the overall multilayer satellite system. Specifically, we study the problem of jointly optimizing the GEO/LEO precoders and message splits to maximize the minimum rate among User Terminals (UTs) subject to a transmit power constraint at all satellites. A robust algorithm is proposed to solve the original non-convex optimization problem. Numerical results demonstrate the effectiveness and robustness towards network load and CSI uncertainty of our proposed D-RSMA scheme. Benefiting from the interference management capability, D-RSMA provides significant max-min fairness performance gains compared to several benchmark schemes.

Index Terms—RSMA, max-min fairness, beamforming design, statistical CSIT and CSIR, satellite communication.

I. INTRODUCTION

Low Earth Orbit (LEO) satellite is envisioned as an appealing technique to support and enhance 5G New Radio (NR) and beyond-5G communications [1], [2]. It has benefits in enabling network scalability, reinforcing the communication service availability and reliability, and boosting the performance of limited terrestrial networks in un-served/underserved areas [3], [4]. LEO constellations formed by LEO satellites are required to provide worldwide and continuous coverage. Due to the limited frequency resource, however, different satellite constellations should work in the same frequency band, which

induces mutual interference and further destabilizes the reliability of space-to-ground links, especially in Geostationary Orbit (GEO)-LEO coexisting scenarios [5], [6].

To manage the mutual interference, some existing works [5]–[7] study the power controlling-based methods. On the one hand, the authors in [7] studied the GEO and LEO coexistence system where the LEO satellites serve as primary and the GEO satellite acts as secondary. Beam hopping and adaptive power control techniques are implemented at the GEO satellite to maximize the system throughput and minimize the interference from GEO to the LEO network. On the other hand, the authors of [5] and [6] considered a case where the GEO satellite is treated as primary and the LEO as secondary. [5] focused on a single GEO-single LEO co-existing system, and the authors formulated a beam power control problem solved by a fractional programming algorithm aiming to maximize the LEO transmission rate while satisfying the service quality requirement of the GEO satellite. Further, [6] extended the scenario to a single GEO-multiple LEO satellites network, a flexible spectrum sharing and cooperative communication method is proposed to mitigate the inter-system interference, where LEO users can be served by multiple LEO satellites cooperatively.

In contrast to the works [5]–[7] that concentrate on power control in non-terrestrial networks, beamforming techniques can also be utilized to coordinate the interference between different satellite systems and improve system performance. Specifically, Rate Splitting Multiple Access (RSMA), relying on linear precoding rate-splitting at the transmitter and Successive Interference Cancellation (SIC) at the receivers, has emerged as a promising multiple access technique for modern multi-antenna networks [8]. RSMA divides user messages into common and private parts at the transmitter. The common parts of the split messages are combined and encoded into a common stream, then decoded by multiple users, while the private parts are encoded separately and decoded by their corresponding users (and treated as noise by co-scheduled users) [9]–[11]. There are various structures of RSMA, including 1-layer RSMA, multilayer (hierarchical) RSMA, and generalized RSMA. The gains of RSMA have been demonstrated in various multi-antenna terrestrial networks in terms of energy efficiency [12], [13], user fairness [14], [15], robustness and latency [16]–[19] for a wide range of network loads and user channel conditions.

More recently, building upon the promising gains offered by RSMA in multigroup multicast [20], several works extended the application of RSMA to satellite communications [21],

Y. Xu and L. Yin are with the Communications and Signal Processing Group, Department of Electrical and Electronic Engineering, Imperial College London, London SW7 2AZ, U.K. (email: yunnuo.xu19, longfei.yin17@imperial.ac.uk).

Y. Mao is with the School of Information Science and Technology, ShanghaiTech University, Shanghai 201210, China (email: maoyj@shanghaitech.edu.cn).

W. Shin is with the School of Electrical Engineering, Korea University, Seoul 02841, South Korea (email: wjshin@korea.ac.kr).

B. Clerckx is with the Department of Electrical and Electronic Engineering at Imperial College London, London SW7 2AZ, UK and with Silicon Austria Labs (SAL), Graz A-8010, Austria (email: b.clerckx@imperial.ac.uk).

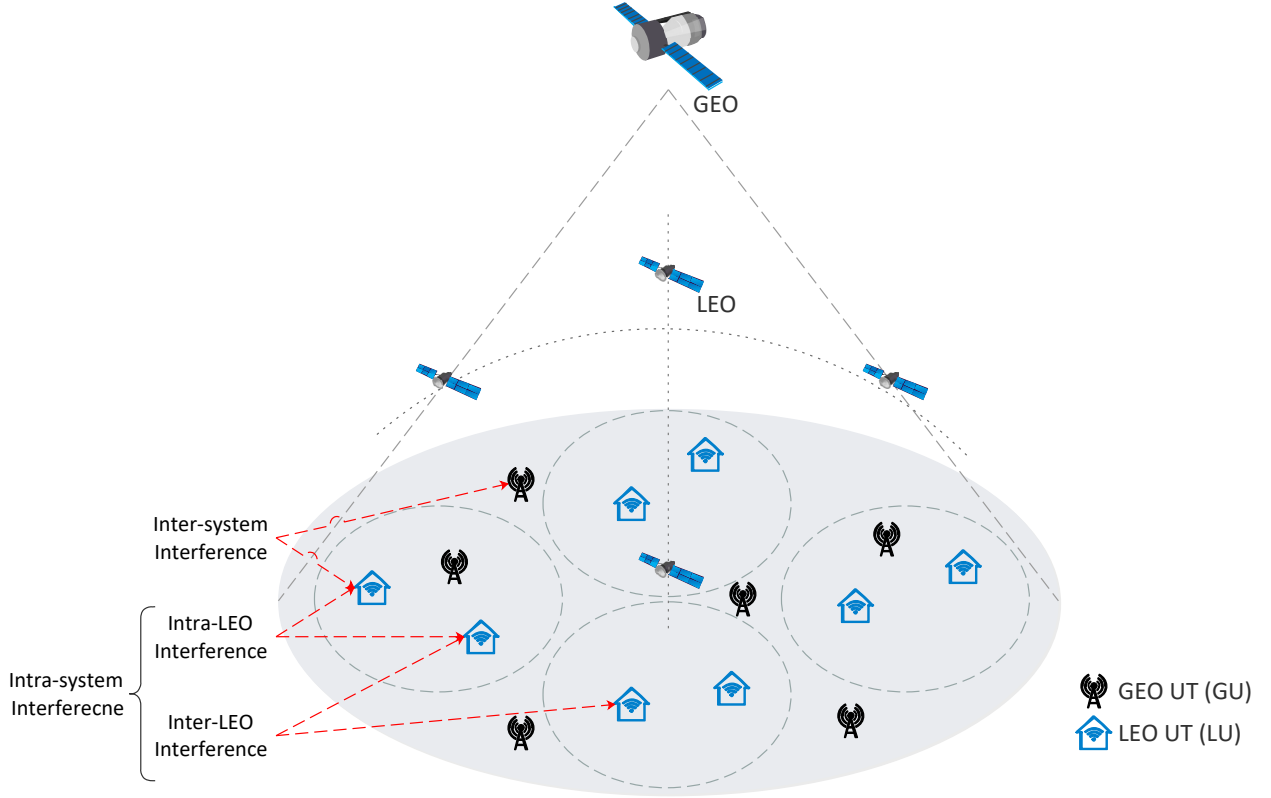


Fig. 1. Multilayered satellite system model with 1 GEO satellite and 4 LEO satellites, $N = 6$, $K = 8$.

[22] and the Satellite-Terrestrial Integrated Network (STIN) [23], [24]. Specifically, [21] implemented RSMA in a two-beam GEO satellite communication system to mitigate the inter-beam interference and improve the achievable rate region. [22] considered an RSMA-based multibeam multicast network with different Channel State Information at Transmitter (CSIT) qualities, in which a Weighted Minimum-Mean Square Error (WMMSE)-based algorithm was proposed to maximize the Max-Min Fairness (MMF) ergodic rate. A general STIN framework was presented in [23], [24], in which the mutual interference between satellite users and cellular ones is taken into account. The authors designed two RSMA-based STIN schemes to suppress interference aiming to maximize the minimum fairness rate among all satellite users and cellular users. Simulation results showed that the proposed scheme achieves higher MMF rate than the conventional schemes without RSMA, illustrating the effectiveness of RSMA to manage the interference among satellites.

However, [21]–[24] consider GEO-only or STIN network and do not investigate multiple orbit constellations co-existence network. There is limited work which investigated a single-GEO-single LEO satellite network [25], where the GEO satellite adopted Orthogonal Multiple Access (OMA) and the LEO employed RSMA-based multigroup multicast transmission. In [25], a GEO satellite serves as primary network while LEO operates as secondary network. RSMA is used to mitigate the interference and improve the sum rate of LEO users. Nevertheless, [25] does not make full use of RSMA, since it only optimizes the power allocation without beamforming. Besides, it relies on perfect CSIT and Channel

State Information at Receiver (CSIR), which lacks practicality in real-world communication situations.

Motivated by 1) the appealing interference management capability of RSMA and 2) the lack of more comprehensive beamforming and power control strategies in GEO-LEO co-existence networks, we further investigate a multilayer satellite network consisting of a GEO satellite and multiple LEO satellites (as shown in Fig. 1). RSMA is implemented across satellites to manage the interference in and between both sub-networks under imperfect CSIT and CSIR. The contributions of this article are summarized as follows:

- 1) We first present a general framework to manage the interference in GEO-LEO coexistence networks, where RSMA is distributedly implemented, namely Distributed-RSMA (D-RSMA), at both GEO and LEO satellite sub-networks. In this framework, we assume that both satellite systems share the same radio spectrum due to the spectrum scarcity. The gateway is deployed to gather information, allocate resources, and manage interference. This framework differs from prior RSMA STIN papers due to the involvement of multiple LEO satellites, and a distributed implementation strategy of RSMA, i.e., D-RSMA, at both GEO and LEO networks.
- 2) It is difficult to acquire the instantaneous Channel State Information (CSI) in real-world, however, statistical CSI varies slower than instantaneous CSI, which allows it to be relatively accurately and easily captured by both the satellites and User Terminals (UTs). Therefore, we investigate a robust beamforming design for D-RSMA with statistical CSIT and CSIR. To the best of our

knowledge, this is the first work in the literature on joint GEO-LEO beamforming design with imperfect CSIT and CSIR.

- 3) Based on the proposed multilayer D-RSMA framework, we formulate an MMF problem in order to jointly optimize the beamforming and power allocation of GEO and LEO satellites as well as the message splits of RSMA. Instead of focusing on the performance of one of the sub-networks, and maintaining the quality of service for the other sub-network, the objective of this paper is to maximize the minimum rate among all GEO and LEO UTs.
- 4) Due to the nonconvex and mathematical intractable essence of the formulated optimization problem, we transform the original problem into a tractable form by using Semi-Definite Programming (SDP) and first-order Taylor approximation, and then a penalty function-based iterative algorithm is proposed to tackle the optimization problem. Numerical results demonstrate that the proposed D-RSMA scheme is robust to user deployment and channel uncertainty. D-RSMA achieves a MMF rate gain over benchmark schemes.

The rest of this paper is organized as follows. The system model and multilayer D-RSMA scheme are introduced in Section II. The MMF optimization problem and proposed robust SDP-based iterative optimization algorithm are specified in Section III. Simulation results illustrating the effectiveness of our proposed scheme are discussed in Section IV, followed by the conclusions in Section V. The major variables adopted in the paper are listed in Table I for ease of reference.

In the remaining sections of this work, matrices, column vectors, and scalars are denoted by boldface uppercase, boldface lowercase, and standard letters, respectively. The operator $(\cdot)^T$ denotes transpose and $(\cdot)^H$ denotes conjugate-transpose. \circ is Hadamard product. $\lambda_{\max}(\cdot)$ denotes the maximum eigenvalue of the matrix. $\mathcal{CN}(\zeta, \sigma^2)$ represents a complex Gaussian distribution with mean ζ and variance σ^2 . $\text{tr}(\cdot)$ is the trace. $|\cdot|$ is the absolute value and $\|\cdot\|$ is the Euclidean norm. \mathbb{C} denotes the complex space. $|\mathcal{A}|$ is the cardinality of the set \mathcal{A} .

II. SYSTEM MODEL

We consider a multilayer satellite system with a single GEO satellite and M LEO satellites serving N single-antenna GEO UTs (GUs) and K single-antenna LEO UTs (LUs), respectively. GUs are the UTs served by the GEO, and LUs are the UTs served by the LEO satellites. Fig. 1 shows a toy example of the system model with 1 GEO and 4 LEO satellites serving $N = 6$ GUs, and $K = 8$ LUs. We denote the set of LEO satellites as $\mathcal{M} = \{1, \dots, M\}$. $\mathcal{N} = \{1, \dots, N\}$ and $\mathcal{K} = \{1, \dots, K\}$ are the sets of UTs served by GEO and LEO, respectively. LUs are divided into M groups, and \mathcal{K}_m denotes the set of UTs under the coverage of m -th LEO satellite. $\bigcup_{m \in \mathcal{M}} \mathcal{K}_i = \mathcal{K}$, $\mathcal{K}_i \cap \mathcal{K}_j = \emptyset$, $i, j \in \mathcal{M}$, $i \neq j$. The size of the m -th group is $K_m = |\mathcal{K}_m|$, $\forall k \in \mathcal{K}_m$. GEO and LEO satellites are equipped with N_{tg} and N_{tl} feeds array fed reflector antennas, respectively. We assume that the GEO and LEO satellites operate in the same radio spectrum. The

TABLE I
VARIABLE LIST

Notation	Definition
M	number of LEO satellites
N	number of GUs
K	number of LUs
N_{tg}	number of antennas for GEO
N_{tl}	number of antennas for LEO
$\mathbf{h}_{g,n}$	channels between GEO and GU- n
\mathbf{h}_{g2l,k_m}	channels between GEO and LU- k_m
\mathbf{h}_{l,mk_m}	channels between LEO- m and LU- k_m
$\mathbf{h}_{l2g,mn}$	channels between LEO- m and GU- n
$s_{g,c}$	common stream from GEO
$s_{g,d}$	GUs-designated stream from GEO
$s_{l,m}^{sub}$	sub-common stream from LEO- m
s_{p,k_m}	private stream from LEO- m
\mathbf{w}_c	precoders for GEO common
\mathbf{w}_d	precoders for GEO GUs-designated stream
$\mathbf{p}_{c,m}$	precoders for LEO- m sub-common stream
\mathbf{p}_{p,k_m}	precoders for LEO- m private stream

satellites are managed by the gateway (GW)s, which act as a control hub to gather and handle various types of data, apply centralized processing, and oversee the overall system through resource allocation and interference management. We assume that statistical imperfect CSIT and CSIR are available in the network.

Due to the spectrum sharing and co-existence GEO/LEO satellites, each user experiences hierarchical multi-user interference. GUs receive inter-system interference from LEO satellites, besides, LUs suffer from inter-LEO interference from unintended LEO satellites as well as from inter-system interference from GEO. The GEO and LEO satellites can exploit various multiple access techniques to manage the interference, such as RSMA, Space Division Multiple Access (SDMA), multicast [26] etc. Inspired by the state-of-the-art RSMA frameworks and the interference coordination capability of RSMA [11], we propose a scheme where RSMA is distributedly implemented at different satellites, which is denoted as D-RSMA. Different from prior literature which typically deploys traditional RSMA in one network, in this work, the proposed D-RSMA implements RSMA across the networks (i.e., GEO and LEO sub-networks), enhancing the ability of interference management. In this section, we first elaborate the received signal by GUs and LUs followed by channel models and imperfect channel model. Then we illustrate the signal processing progress at GUs and LUs.

A. Transmit and Received Signal

We assume that all GUs are interested in the same content, and the multicast message G is split into a common part, G_c , and a GUs-designated part, G_d , in D-RSMA scheme. The unicast messages L_1, \dots, L_{K_m} for LUs served by the m -th LEO are split into three parts, namely, a super-common part, a sub-common part and a private part, i.e., $L_{k_m} \rightarrow$

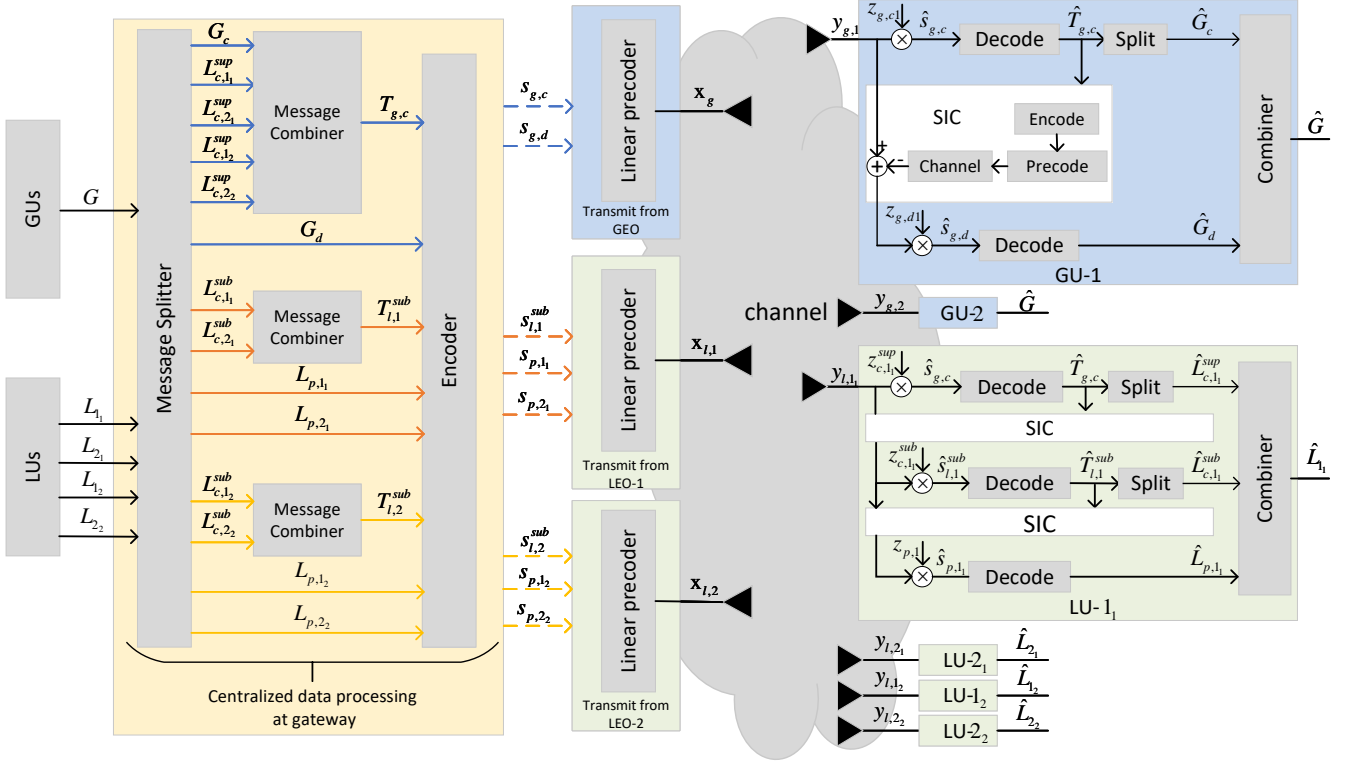


Fig. 2. D-RSMA signal transmission model for 1 GEO and 2 LEO satellites deployment, $N = 2$, $M = 4$, each LEO satellite serves 2 LUs.

$\{L_{c,k_m}^{sup}, L_{c,k_m}^{sub}, L_{p,k_m}\}$, $\forall k_m \in \mathcal{K}_m$, $m \in \mathcal{M}$. The superscript “sup” and “sub” are used to represent the super-common and sub-common parts for LUs messages/streams, respectively. The common message for GUs, G_c , and all super-common messages for LUs, $\{\bigcup_{k_m \in \mathcal{K}} L_{c,k}^{sup}\}$, are combined as $T_{g,c}$ and encoded into $s_{g,c}$ to be transmitted from GEO and decoded by all GUs and LUs. It manages the inter-system interference between GEO and LEO so as the inter-LEO interference. The GUs-designated message, G_d , is encoded into $s_{g,d}$. The vector of GEO streams is $\mathbf{s}_g = [s_{g,c}, s_{g,d}]^T$ and $\mathbb{E}\{\mathbf{s}_g \mathbf{s}_g^H\} = \mathbf{I}$. The sub-common messages, $\{\bigcup_{k_m \in \mathcal{K}_m} L_{c,k_m}^{sub}\}$, for LUs under m -th LEO coverage are combined into a sub-common message $T_{l,m}^{sub}$ and encoded into a sub-common stream $s_{l,m}^{sub}$ to manage the intra-LEO interference. The private parts for LUs are independently encoded into private streams $s_{p,1}, \dots, s_{p,K_m}$. The vector of m -th LEO satellite streams $\mathbf{s}_{l,m} = [s_{l,m}^{sub}, s_{p,1}, \dots, s_{p,K_m}]^T \in \mathbb{C}^{(K_m+1) \times 1}$ is obtained, and we assume it satisfies $\mathbb{E}\{\mathbf{s}_{l,m} \mathbf{s}_{l,m}^H\} = \mathbf{I}$. A signal transmission model for D-RSMA is shown in Fig. 2.

Data streams are mapped to the transmit antennas via precoding matrix $\mathbf{W} = [\mathbf{w}_c, \mathbf{w}_d] \in \mathbb{C}^{N_{tg} \times 2}$ at GEO satellite and precoding matrices $\mathbf{P}_m = [\mathbf{p}_{c,m}, \mathbf{p}_{p,1}, \dots, \mathbf{p}_{p,K_m}]$ at m -th LEO satellite, where $\mathbf{P}_m \in \mathbb{C}^{N_{tl} \times (K_m+1)}$. The respective transmit signals at the GEO and m -th LEO are

$$\mathbf{x}_g = \mathbf{w}_c s_{g,c} + \mathbf{w}_d s_{g,d}, \quad (1a)$$

$$\mathbf{x}_{l,m} = \mathbf{p}_{c,m} s_{l,m}^{sub} + \sum_{k=m}^{K_m} \mathbf{p}_{p,k} s_{p,k}, \quad m \in \mathcal{M}. \quad (1b)$$

Following [27], [28], we assume that they are subject to the total power constraints, i.e., $\mathbb{E}\{\mathbf{x}_g^H \mathbf{x}_g\} \leq P_g$, and $\mathbb{E}\{\mathbf{x}_{l,m}^H \mathbf{x}_{l,m}\} \leq P_l$. The received signal at GUs and LUs are illustrated in the following two subsections, respectively.

1) *GEO UT received signal*: After each GEO UT (GU) receives the signal, it first decodes the GEO common stream, $s_{g,c}$, by treating other streams as noise. The interference between GEO and LEO satellites and inter-LEO interference are handled by $s_{g,c}$, because it contains a portion of UT messages from both GUs and LUs. Each GU or LEO UT (LU) partially decodes the inter-system interference and partially treats inter-system interference as noise, so as inter-LEO interference for LUs. The signal received at GU- n can be expressed as

$$\begin{aligned} y_{g,n} &= \mathbf{h}_{g,n}^H \mathbf{x}_g + \sum_{m=1}^M \mathbf{h}_{l2g,mn}^H \mathbf{x}_{l,m} + n_n \\ &= \underbrace{\mathbf{h}_{g,n}^H \mathbf{w}_c s_{g,c} + \mathbf{h}_{g,n}^H \mathbf{w}_d s_{g,d}}_{\text{Desired signal}} \\ &\quad + \underbrace{\sum_{m=1}^M \mathbf{h}_{l2g,mn}^H (\mathbf{p}_{c,m} s_{l,m}^{sub} + \sum_{i=1}^{K_m} \mathbf{p}_{p,i} s_{p,i})}_{\text{Interference from LEO satellites}} + n_n, \end{aligned} \quad (2)$$

where $\mathbf{h}_{g,n} \in \mathbb{C}^{N_{tg} \times 1}$ is the channel between the GEO satellite and GU- n and $\mathbf{h}_{l2g,mn} \in \mathbb{C}^{N_{tl} \times 1}$ is the channel between the m -th LEO satellite and GU- n , $m \in \mathcal{M}$. $n_n \sim \mathcal{CN}(0, \sigma_n^2)$ represents the Additive White Gaussian Noise (AWGN) at GU- n , $n \in \mathcal{N}$.

2) *LEO UT received signal*: The received signal at LU- k_m writes as

$$\begin{aligned}
 y_{l,k_m} &= \mathbf{h}_{l,mk_m}^H \mathbf{x}_{l,m} + \mathbf{h}_{g2l,k_m}^H \mathbf{x}_g + \sum_{\substack{j=1, \\ j \neq m}}^M \mathbf{h}_{l,jk_m}^H \mathbf{x}_{l,j} + n_{k_m} \\
 &= \underbrace{\mathbf{h}_{g2l,k_m}^H \mathbf{w}_{csg,c} + \mathbf{h}_{l,mk_m}^H \mathbf{p}_{c,m} s_{l,m}^{sub} + \mathbf{h}_{l,mk_m}^H \mathbf{p}_{p,k_m} s_{p,k_m}}_{\text{Desired signal}} \\
 &\quad + \underbrace{\mathbf{h}_{l,mk_m}^H \sum_{\substack{i=1, \\ i \neq k_m}}^{K_m} \mathbf{p}_{p,i} s_{p,i}}_{\text{Intra-LEO interference}} + \underbrace{\mathbf{h}_{g2l,k_m}^H \mathbf{w}_{dsg,d}}_{\text{Interference from GEO satellite}} \\
 &\quad + \underbrace{\sum_{\substack{j=1, \\ j \neq m}}^M \mathbf{h}_{l,jk_m}^H \left(\mathbf{p}_{c,j} s_{l,j}^{sub} + \sum_{i=1}^{K_j} \mathbf{p}_{p,i} s_{p,i} \right)}_{\text{Inter-LEO interference}} + n_{k_m}, \tag{3}
 \end{aligned}$$

where $\mathbf{h}_{l,mk_m} \in \mathbb{C}^{N_{tl} \times 1}$ is the channel between the m -th LEO satellite and LU- k_m and $\mathbf{h}_{g2l,k_m} \in \mathbb{C}^{N_{tg} \times 1}$ is the channel between the GEO satellite and LU- k_m . $n_{k_m} \sim \mathcal{CN}(0, \sigma_{k_m}^2)$ represents the AWGN at LU- k_m , $k_m \in \mathcal{K}_m$, $m \in \mathcal{M}$.

B. Channel Model

In this subsection, we illustrate the channel models of GEO and LEO satellites.

1) *GEO Satellite Channel*: We assume that the channel realizations between the satellite and different UTs are uncorrelated, because different UTs are often geographically separated by a certain distance. The main characteristics of GEO channel include atmospheric fading and radiation pattern. Rain attenuation is the dominant atmospheric impact for the Ka-band satellite channel, and it is often characterized by a lognormal distribution [22], [23]. The GEO satellite channel vector between the satellite and i -th UT is expressed as $\mathbf{h}_{g,i} = [h_{g,1i}, h_{g,2i}, \dots, h_{g,N_{ti}i}]^T$, $i \in \mathcal{N} \cup \mathcal{K}$. The n_{tg} -th entry of the channel between the GEO satellite and the UT- i can be written as

$$h_{g,n_{tg}i} = \frac{\sqrt{G_r G_{g,i}}}{4\pi \frac{d_{g,i}}{\lambda} \sqrt{\kappa T_{sys} B_w}} \chi_{n_{tg}i}^{-\frac{1}{2}} e^{-j\phi_{g,n_{tg}i}}, i \in \{\mathcal{N} \cup \mathcal{K}\}, \tag{4}$$

where G_r and $G_{g,i}$ are the UT antenna gain and the antenna gain from GEO satellite to the UT- i , respectively. $d_{g,i}$ and λ denote the distance from the GEO satellite to UT- i and the carrier wavelength, respectively. κ is the Boltzmann constant, T_{sys} is the receiving system noise temperature and B_w denotes the user link bandwidth. The large-scale fading is modeled as $\chi_{n_{tg}i,dB} = 10 \log_{10}(\chi_{n_{tg}i})$, and $\ln(\chi_{n_{tg}i,dB}) \sim \mathcal{N}(\mu, \sigma)$. $\phi_{g,i} = [\phi_{g,1i}, \phi_{g,2i}, \dots, \phi_{g,N_{ti}i}]^T \in \mathbb{R}^{N_{tg} \times 1}$ is channel phase vector. $G_{g,i}$ can be further expressed as

$$G_{g,i} = G_{max} \left[\frac{J_1(u_{g,i})}{2u_{g,i}} + 36 \frac{J_3(u_{g,i})}{u_{g,i}^3} \right]^2, \tag{5}$$

where $u_{g,i} = 2.07123 \frac{\sin(\theta_{g,i})}{\sin(\theta_{3dB})}$. $\theta_{g,i}$ is the angle between UT- i and the center of GEO satellite beam. θ_{3dB} denotes

a 3 dB loss angle compared with the beam center. G_{max} is the maximum beam gain of the beam center. J_1 and J_3 are first-kind Bessel functions with first-order and third-order, respectively. The channel between GEO and LU- k_m is $\mathbf{h}_{g2l,k_m} = [h_{g,1k_m}, h_{g,2k_m}, \dots, h_{g,N_{tg}k_m}]^T$, $k_m \in \mathcal{K}_m$, $m \in \mathcal{M}$.

2) *LEO Satellite Channel*: Due to the high mobility of LEO, the propagation characteristics of satellite channel and impact on the channel modelling are different. It differs from GEO satellite channel due to the Doppler shift and delay [28], [29]. The Doppler shift $f_{i,u}$ associated with propagation path u of UT- i is dominated by two independent Doppler shifts, $f_{i,u}^{sat}$ and $f_{i,u}^{ut}$, which result from the movements of LEO satellite and UT, respectively. The channel between m -th LEO satellite and i -th UT is

$$\mathbf{h}_{l,mi} = g_{mi}(t, f) e^{j2\pi(f_{i,u}^{sat} t - f_{i,u}^{min})} e^{-j\phi_{l,mi}}, \tag{6a}$$

$$g_{mi}(t, f) = \sum_{u=0}^{U_i-1} g_{i,u} e^{j2\pi(f_{i,u}^{ut} t - f_{i,u}^{ut})}, i \in \{\mathcal{N} \cup \mathcal{K}\}, \tag{6b}$$

where τ_i^{min} is the minimum value of the propagation delays of the i -th UT defined by $\tau_i^{min} = \min_u \{\tau_{i,u}\}$, where $\tau_{i,u}$ is the delay of the u -th path to UT- i . We denote the delay difference of UT- i with path u as $\tau_{i,u}^{ut} \triangleq \tau_{i,u} - \tau_i^{min}$. U_i denotes the number of propagation paths of the i -th UT. The Doppler shift $f_{i,u}^{sat}$ induced by the movement of the LEO satellite can be considered to be identical for different propagation paths of the same UT- i due to the relatively high altitude of the LEO satellite [29], [30]. Hence, in order to simplify the notation, we recast and omit the path index the Doppler shifts caused by the motion of the LEO satellite as $f_{i,u}^{sat} = f_i^{sat}$. $\phi_{l,mi}$ is the channel angle vector from LEO satellite- m to UT- i . $\phi_{l,mi} = [\phi_{1i}^{l,m}, \phi_{2i}^{l,m}, \dots, \phi_{N_{ti}i}^{l,m}]^T \in \mathbb{R}^{N_{tl} \times 1}$ is channel phase vector, and it can be calculated by using geographic location information between the i -th UT and the LEO satellite, or it can be acquired through using satellite positioning system [31]. $g_{mi}(t, f)$ is LEO satellite downlink channel gain, $g_{i,u}$ is the complex-valued gain corresponding to path u and UT- i [32]. LEO satellite system usually operates under Line-of-Sight (LoS) propagations, and we assume $g_{mi}(t, f)$ follows Rician fading distribution with the Rician factor κ_i and power

$$\gamma_i = \mathbb{E} \left\{ |g_i(t, f)|^2 \right\} = \frac{G_r G_l}{(4\pi \frac{d_{mi}}{\lambda})^2 \kappa T_{sys} B_w}, \tag{7}$$

where G_l is the antenna gain of the LEO satellite. Alternatively, the real and imaginary parts of $g_{mi}(t, f)$ have independent and identically distributed (i.i.d) real-valued Gaussian entries with a certain mean and variance, i.e., $g_{mi}(t, f) \sim \mathcal{N} \left(\sqrt{\frac{\kappa_i \gamma_i}{2(\kappa_i + 1)}}, \frac{\gamma_i}{2(\kappa_i + 1)} \right)$. Following [29], [33], we assume that the time and frequency compensation can be properly performed at UTs. Specifically, the Doppler compensation, $f_i^{syn} = f_i^{sat}$, and delay compensation, $\tau_i^{syn} = \tau_i^{min}$ are applied.

C. Imperfect channel

Due to the long propagation delay between a satellite and UTs as well as the mobility of satellites and UTs, it is difficult

to obtain instantaneous CSI. Hence, we assume that statistical CSIT and CSIR are available in the network.

Under imperfect CSIT scenario, we utilize ergodic rate as a long-term measurement to capture the expected performance over a known statistical channel distribution. With imperfect CSIR deployment, the progress of SIC is effected and the stream cannot be perfectly removed, since UTs lack of accurate channel information. We denote GEO channel phase vector $\phi_{g,i}$ as the sum of a estimated angle, $\hat{\phi}_{g,i}$, and estimation error, $\phi_{eg,i}$, i.e., $\phi_{g,i} = \hat{\phi}_{g,i} + \phi_{eg,i}$, $i \in \mathcal{N} \cup \mathcal{K}$ [4]. The angle estimation error is characterized by an normal distribution $\phi_{eg,i} \sim \mathcal{N}(\mathbf{0}, \sigma_{e,g}^2 \mathbf{I})$. Then, the relationship between the actual channel and estimated channel can be expressed as $\mathbf{h}_{g,i} = \hat{\mathbf{h}}_{g,i} \circ \Phi_{eg,i}$, where $\Phi_{eg,i} = \exp(-j\phi_{eg,i})$. Similarly, the m -th LEO channel phase vector can be written as $\phi_{l,mi} = \hat{\phi}_{l,mi} + \phi_{el,mi}$, where $\phi_{el,mi} \sim \mathcal{N}(\mathbf{0}, \sigma_{e,l}^2 \mathbf{I})$. The channel vector from m -th LEO satellite to i -th UT is $\mathbf{h}_{l,mi} = \hat{\mathbf{h}}_{l,mi} \circ \Phi_{el,mi}$, where $\Phi_{el,mi} = \exp(-j\phi_{el,mi})$. $\phi_j = \mathbf{0}$, $j \in \{eg, i\}, \{el, mi\}$, represents perfect CSI.

D. Signal transmission and rate expressions

In this subsection, the signal transmission progress, Signal to Interference plus Noise Ratio (SINR) and ergodic rate expressions are illustrated.

1) *GEO UT*: Once receiving the signal, GU- n first decodes the common stream $s_{g,c}$. Under imperfect CSIR, UTs only have statistical CSI, therefore, UTs decode the desired stream based on the estimated channel [34]. The SINR of decoding the common stream at GU- n is expressed as

$$\rho_{g,cn} = \frac{\hat{S}_{g,cn}}{\tilde{S}_{g,cn} + S_{g,dn} + I_{g,n}^{tot} + \sigma_n^2}, \quad n \in \mathcal{N}, \quad (8)$$

where $\hat{S}_{g,cn} = |\hat{\mathbf{h}}_{g,n}^H \mathbf{w}_c|^2$ and $S_{g,dn} = |\mathbf{h}_{g,n}^H \mathbf{w}_d|^2$. $\tilde{S}_{g,cn} = |\mathbf{h}_{g,n}^H \mathbf{w}_c|^2 - |\hat{\mathbf{h}}_{g,n}^H \mathbf{w}_c|^2$ is residual power. $I_{g,n}^{tot} = \sum_{m=1}^M |\mathbf{h}_{l2g,mn}^H \mathbf{p}_{c,m}|^2 + \sum_{m=1}^M \sum_{i=1}^{K_m} |\mathbf{h}_{l2g,mn}^H \mathbf{p}_{p,i}|^2$ is the sum of interference power of sub-common streams and the private streams for LUs. The corresponding ergodic rate expresses as $R_{g,cn} = \mathbb{E}\{\log_2(1 + \rho_{g,cn})\}$. The received signal after decoding $s_{g,c}$ writes as

$$\begin{aligned} y_{g,n}^{SIC} &= y_{g,n} - \hat{\mathbf{h}}_{g,n}^H \mathbf{w}_c \\ &= \hat{\mathbf{h}}_{g,n}^H (\text{diag}(\Phi_{eg,n}^H) - \mathbf{I}) \mathbf{w}_c s_{g,c} + \mathbf{h}_{g,n}^H \mathbf{w}_d s_{g,d} \\ &\quad + \sum_{m=1}^M \mathbf{h}_{l2g,mn}^H (\mathbf{p}_{c,m} s_{l,m}^{sub} + \sum_{i=1}^{K_m} \mathbf{p}_{p,i} s_{p,i}) + n_n \\ &= \tilde{\mathbf{h}}_{g,n}^H \mathbf{w}_c s_{g,c} + \mathbf{h}_{g,n}^H \mathbf{w}_d s_{g,d} \\ &\quad + \sum_{m=1}^M \mathbf{h}_{l2g,mn}^H (\mathbf{p}_{c,m} s_{l,m}^{sub} + \sum_{i=1}^{K_m} \mathbf{p}_{p,i} s_{p,i}) + n_n, \end{aligned} \quad (9)$$

where $\tilde{\mathbf{h}}_{g,n}^H$ is denoted as residual channel in this paper. Hence, $\tilde{S}_{g,cn}$ can be rewritten as $\tilde{S}_{g,cn} = |\tilde{\mathbf{h}}_{g,n}^H \mathbf{w}_c|^2$.

Subsequently, GU- n decodes the GUs-designated stream $s_{g,d}$. Accordingly, GU- n 's decoding SINR of the GUs-designated stream writes as

$$\rho_{g,dn} = \frac{\hat{S}_{g,dn}}{\tilde{S}_{g,cn} + \tilde{S}_{g,dn} + I_{g,n}^{tot} + \sigma_n^2}, \quad n \in \mathcal{N}, \quad (10)$$

where $\tilde{S}_{g,dn}$ is the residual power of decoding $s_{g,d}$, and $\tilde{S}_{g,dn} = |\tilde{\mathbf{h}}_{g,n}^H \mathbf{w}_d|^2$. The ergodic designated rate of GU- n is expressed as $R_{g,dn} = \mathbb{E}\{\log_2(1 + \rho_{g,dn})\}$. GU- n reconstructs the original message after the common and GUs-designated messages have been decoded by taking the decoded G_c from the decoded $T_{g,c}$ and combining it with the decoded G_d .

2) *LEO UT*: Based on estimated channel, LU- k_m firstly decodes the $s_{g,c}$ by treating other interference as noise. The corresponding SINR is

$$\rho_{l,k_m}^{sup} = \frac{\hat{S}_{g2l,ck_m}}{\tilde{S}_{g2l,ck_m} + S_{l,ck_m} + S_{l,pk_m} + I_{l,k_m}^{tot} + \sigma_{k_m}^2}, \quad k_m \in \mathcal{K}_m, \quad (11)$$

where $\hat{S}_{g2l,ck_m} = |\hat{\mathbf{h}}_{g2l,k_m}^H \mathbf{w}_c|^2$, $\tilde{S}_{g2l,ck_m} = |\tilde{\mathbf{h}}_{g2l,k_m}^H \mathbf{w}_c|^2$, $S_{l,ck_m} = |\mathbf{h}_{l,mk_m}^H \mathbf{p}_{c,m}|^2$, $S_{l,pk_m} = |\mathbf{h}_{l,mk_m}^H \mathbf{p}_{p,k_m}|^2$. $\tilde{\mathbf{h}}_{g2l,k_m}^H = \hat{\mathbf{h}}_{g2l,k_m}^H (\text{diag}(\Phi_{eg,k_m}^H) - \mathbf{I})$ denotes the residual channel between GEO satellite and LU- k_m . $I_{l,k_m}^{tot} = \sum_{i=1, i \neq k_m}^{K_m} |\mathbf{h}_{l,mk_m}^H \mathbf{p}_{p,i}|^2 + \sum_{j=1, j \neq m}^M |\mathbf{h}_{l,jk_m}^H \mathbf{p}_{c,j}|^2 + \sum_{j=1, j \neq m}^M \sum_{i=1}^{K_j} |\mathbf{h}_{l,jk_m}^H \mathbf{p}_{p,i}|^2 + |\mathbf{h}_{g2l,k_m}^H \mathbf{w}_d|^2$ is the sum of interference power received at LU- k_m . The corresponding ergodic rate is $R_{l,k_m}^{sup} = \mathbb{E}\{\log_2(1 + \rho_{l,k_m}^{sup})\}$. In order to make sure that all GUs and LUs can decode $s_{g,c}$, we define the common rate

$$R_c = \min_{n \in \mathcal{N}, k \in \mathcal{K}} \{R_{g,cn}, R_{l,k}^{sup}\}. \quad (12)$$

Since $s_{g,c}$ is shared among all GUs and LUs, we define $R_c \triangleq \sum_{n=1}^N C_{g,n} + \sum_{m=1}^M \sum_{k_m=1}^{K_m} C_{l,k_m}^{sup}$, where $C_{g,n}$ and C_{l,k_m}^{sup} denote the n -th GU's and k_m -th LU's portions of common rate, respectively.

Once $s_{g,c}$ is decoded, its contribution to the original received signal y_{l,k_m} is subtracted through SIC. After that, LU- k_m decodes its sub-common stream $s_{l,m}^{sub}$ by treating other sub-common streams as noise. The sub-common streams are used to manage intra-LEO interference since it contains parts of messages for LUs served by the same LEO. Sub-common streams enable users to partially decode intra-LEO interference and partially treat intra-LEO interference as noise. The SINR of decoding the sub-common stream $s_{l,m}^{sub}$ at LU- k_m served by LEO- m is

$$\rho_{l,k_m}^{sub} = \frac{\hat{S}_{l,ck_m}}{\tilde{S}_{g2l,ck_m} + \tilde{S}_{l,ck_m} + S_{l,pk_m} + I_{l,k_m}^{tot} + \sigma_{k_m}^2}, \quad k_m \in \mathcal{K}_m, \quad (13)$$

where $\tilde{S}_{l,ck_m} = |\tilde{\mathbf{h}}_{l,mk_m}^H \mathbf{p}_{c,m}|^2$. $\tilde{\mathbf{h}}_{l,mk_m}^H = \hat{\mathbf{h}}_{l,mk_m}^H (\text{diag}(\Phi_{el,mk_m}^H) - \mathbf{I})$ is the residual channel between LEO satellite m and LU- k_m . The ergodic rate of the sub-common stream is $R_{l,k_m}^{sub} = \mathbb{E}\{\log_2(1 + \rho_{l,k_m}^{sub})\}$. To guarantee that all LUs served by m -th LEO are capable of decoding $s_{l,m}^{sub}$, we define the achievable sub-common rates as

$$R_{c,m}^{sub} = \min_{k_m \in \mathcal{K}_m} \{R_{l,k_m}^{sub}\} = \sum_{k_m=1}^{K_m} C_{l,k_m}^{sub}, \quad (14)$$

where C_{l,k_m}^{sub} is the rate at which s_{l,k_m}^{sub} is communicated. After the sub-common stream is decoded, re-encoded, precoded, and subtracted from the received signal through SIC, LU- k_m decodes its private stream s_{k_m} . The SINR of decoding the private stream s_{k_m} at LU- k_m is

$$\rho_{k_m} = \frac{\hat{S}_{l,pk_m}}{\tilde{S}_{g2l,ck_m} + \tilde{S}_{l,ck_m} + \tilde{S}_{l,pk_m} + I_{l,k_m}^{tot} + \sigma_{k_m}^2}, \quad k_m \in \mathcal{K}_m, \quad (15)$$

where $\tilde{S}_{l,pk_m} = |\tilde{\mathbf{h}}_{l,mk_m}^H \mathbf{p}_{p,k_m}|^2$. The corresponding ergodic private rate is $R_{p,k_m} = \mathbb{E}\{\log_2(1 + \rho_{k_m})\}$. Thus, the achievable rates of GU- n and LU- k_m are respectively given as

$$R_n = C_{g,n} + R_{g,dn}, \quad n \in \mathcal{N}, \quad (16a)$$

$$R_{k_m} = C_{l,k_m}^{sup} + C_{l,k_m}^{sub} + R_{p,k_m}, \quad k_m \in \mathcal{K}_m, \quad m \in \mathcal{M}. \quad (16b)$$

Remark 1: D-RSMA is designed for managing interference of the co-existence GEO/LEO satellites multilayer network. Each GU decodes $s_{g,c}$ first and requires 1 layer of SIC to decode $s_{g,d}$. By decoding $s_{g,c}$, the inter-system interference can be suppressed since partial inter-system interference is decoded and part of inter-system interference is treated as noise. While each LU requires 2 layers of SIC before decoding intended private stream (in order to decode $s_{g,c}$ first and then decode $s_{l,m}^{sub}$). The inter-system interference and inter-LEO interference is managed through $s_{g,c}$, and the intra-LEO interference is managed by $s_{l,m}^{sub}$.

D-RSMA is a general framework of multilayer network that encompasses traditional RSMA and SDMA as special cases. By switching off $s_{g,c}$, the multiple access technique of GEO sub-network becomes traditional multicasting, and the multiple access approach of LEO sub-network reduces to 1-layer RSMA. By turning off $s_{g,c}$ and sub-common streams, GEO and LEO sub-networks work in multicasting and SDMA manner, respectively.

III. PROBLEM FORMULATION AND PROPOSED ALGORITHM

In this section, we focus on designing a joint optimization of GEO-LEO beamforming problem that maximizes the minimum fairness rate across all GUs and LUs under the constraint of transmit power at all satellites. For D-RSMA based multilayer satellite network, the optimization problem can be formulated as

$$\mathcal{P}_1 : \max_{\mathbf{c}, \mathbf{W}, \mathbf{P}} \min_{n \in \mathcal{N}, k \in \mathcal{K}} \{R_n, R_k\} \quad (17a)$$

$$\text{s.t.} \quad \sum_{n \in \mathcal{N}} C_{g,n} + \sum_{k \in \mathcal{K}} C_{l,k_m}^{sup} \leq R_c \quad (17b)$$

$$\sum_{k_m \in \mathcal{K}_m} C_{l,k_m}^{sub} \leq R_{c,m}^{sub}, \quad m \in \mathcal{M} \quad (17c)$$

$$\text{tr}(\mathbf{W}\mathbf{W}^H) \leq P_g \quad (17d)$$

$$\text{tr}(\mathbf{P}_m \mathbf{P}_m^H) \leq P_l, \quad m \in \mathcal{M} \quad (17e)$$

$$\mathbf{c} \succeq \mathbf{0}, \quad (17f)$$

where $\mathbf{P} = [\mathbf{P}_1, \dots, \mathbf{P}_M]$ represents the precoding matrix at all LEO satellites. $\mathbf{c} = [\mathbf{c}_g, \mathbf{c}_l^{sup}, \mathbf{c}_l^{sub}]$, where $\mathbf{c}_g = [C_{g,1}, \dots, C_{g,N}]^T$, $\mathbf{c}_l^{sup} = [C_{l,1}^{sup}, \dots, C_{l,K}^{sup}]^T$, and $\mathbf{c}_l^{sub} = [C_{l,1}^{sub}, \dots, C_{l,K}^{sub}]^T$ are the vectors of common rate portions. (17b) ensures that all GUs and LUs can successfully decode the common stream $s_{g,c}$. Similarly, (17c) guarantees that the sub-common stream $s_{l,m}^{sub}$ can be decoded by all LUs under the coverage of LEO- m . (17d) and (17e) represent power

constraints of the GEO and LEO satellites. (17f) ensure that all common rate portions are non-negative.

The formulated problem (17) is nonconvex, while it can be transformed into a tractable SDP problem and solved with rank-one constraints. We propose a robust SDP-based iterative optimization algorithm to solve the problem with statistical CSIT and CSIR in this work. Denote $\boldsymbol{\alpha} = \{\boldsymbol{\alpha}_{g,c}, \boldsymbol{\alpha}_{g,p}, \boldsymbol{\alpha}_l^{sup}, \boldsymbol{\alpha}_l^{sub}, \boldsymbol{\alpha}_p\}$ and $\mathbf{F} = \{\mathbf{F}_{g,c}, \mathbf{F}_{g,d}, \mathbf{F}_{l,cm}, \mathbf{F}_{l,pk}|k \in \mathcal{K}, m \in \mathcal{M}\}$, where $\mathbf{F}_{g,c} = \mathbf{w}_c \mathbf{w}_c^H$, $\mathbf{F}_{g,d} = \mathbf{w}_d \mathbf{w}_d^H$, $\{\mathbf{F}_{l,cm} = \mathbf{p}_{c,m} \mathbf{p}_{c,m}^H | m \in \mathcal{M}\}$ and $\{\mathbf{F}_{l,pk} = \mathbf{p}_{l,pk} \mathbf{p}_{l,pk}^H | k \in \mathcal{K}\}$. By introducing auxiliary variables t , $\boldsymbol{\alpha}$ and \mathbf{F} , the equivalent reformulation of \mathcal{P}_1 is

$$\mathcal{P}_2 : \max_{\mathbf{F}, \boldsymbol{\alpha}, \mathbf{c}} t \quad (18a)$$

$$\text{s.t.} \quad t \leq C_{g,n} + \alpha_{g,dn}, \quad n \in \mathcal{N} \quad (18b)$$

$$\sum_{n=1}^N C_{g,n} + \sum_{k=1}^K C_{l,k}^{sup} \leq \alpha_{g,cn}, \quad n \in \mathcal{N} \quad (18c)$$

$$t \leq C_{l,k_m}^{sup} + C_{l,k_m}^{sub} + \alpha_{p,k_m}, \quad k_m \in \mathcal{K}_m, m \in \mathcal{M} \quad (18d)$$

$$\sum_{n=1}^N C_{g,n} + \sum_{k=1}^K C_{l,k}^{sup} \leq \alpha_{l,k_m}^{sup}, \quad k_m \in \mathcal{K}_m, m \in \mathcal{M} \quad (18e)$$

$$\sum_{k_m=1}^{K_m} C_{l,k_m}^{sub} \leq \alpha_{l,k_m}^{sub}, \quad k_m \in \mathcal{K}_m, m \in \mathcal{M} \quad (18f)$$

$$\text{tr}(\mathbf{F}_{g,c}) + \text{tr}(\mathbf{F}_{g,d}) \leq P_g \quad (18g)$$

$$\text{tr}(\mathbf{F}_{l,cm}) + \sum_{k_m=1}^{K_m} \text{tr}(\mathbf{F}_{l,pk_m}) \leq P_l, \quad m \in \mathcal{M} \quad (18h)$$

$$\mathbf{F}_{g,c} \succeq \mathbf{0}, \mathbf{F}_{g,d} \succeq \mathbf{0}, \quad (18i)$$

$$\mathbf{F}_{l,cm} \succeq \mathbf{0}, \quad m \in \mathcal{M} \quad (18j)$$

$$\mathbf{F}_{l,pk_m} \succeq \mathbf{0}, \quad k_m \in \mathcal{K}_m, m \in \mathcal{M} \quad (18k)$$

$$\text{rank}(\mathbf{F}_{g,c}) = 1, \text{rank}(\mathbf{F}_{g,d}) = 1, \quad (18l)$$

$$\text{rank}(\mathbf{F}_{l,cm}) = 1, m \in \mathcal{M} \quad (18m)$$

$$\text{rank}(\mathbf{F}_{l,pk_m}) = 1, \quad k_m \in \mathcal{K}_m, m \in \mathcal{M} \quad (18n)$$

$$\mathbf{c} \succeq \mathbf{0}, \quad (18o)$$

where $\boldsymbol{\alpha}_{g,c} \triangleq [\alpha_{g,c1}, \dots, \alpha_{g,cN}]^T$, $\boldsymbol{\alpha}_{g,p} \triangleq [\alpha_{g,p1}, \dots, \alpha_{g,pN}]^T$, $\boldsymbol{\alpha}_l^{sup} \triangleq [\alpha_{l,1}^{sup}, \dots, \alpha_{l,K}^{sup}]^T$, $\boldsymbol{\alpha}_l^{sub} \triangleq [\alpha_{l,1}^{sub}, \dots, \alpha_{l,K}^{sub}]^T$, $\boldsymbol{\alpha}_p \triangleq [\alpha_{p,1}, \dots, \alpha_{p,K}]^T$ represent the lower bound of corresponding achievable rates. (18g) and (18h) are the equivalent transmit power constraints.

Due to the imperfect CSIT deployment and nonconvex nature of problem (18), we denote

$$\mathbf{H}_{g,n} = \mathbb{E}\{\mathbf{h}_{g,n} \mathbf{h}_{g,n}^H\} \\ = \text{diag}(\hat{\mathbf{h}}_{g,n}) \mathbf{X}_{g,n} \text{diag}(\hat{\mathbf{h}}_{g,n}^H) \quad (19)$$

as symmetric GEO channel matrix, where $\mathbf{X}_{g,n} = \mathbb{E}\{\boldsymbol{\Phi}_{eg,n} \boldsymbol{\Phi}_{eg,n}^H\}$ is the correlation matrix of $\boldsymbol{\Phi}_{eg,n}$. Similarly,

$\mathbf{H}_{l2g,mn}$, \mathbf{H}_{l,mk_m} and \mathbf{H}_{g2l,k_m} are

$$\mathbf{H}_{l2g,mn} = \text{diag}(\hat{\mathbf{h}}_{l2g,mn}) \mathbf{X}_{l,mn} \text{diag}(\hat{\mathbf{h}}_{l2g,mn}^H), \quad (20a)$$

$$\mathbf{H}_{l,mk_m} = \text{diag}(\hat{\mathbf{h}}_{l,mk_m}) \mathbf{X}_{l,mk_m} \text{diag}(\hat{\mathbf{h}}_{l,mk_m}^H), \quad (20b)$$

$$\mathbf{H}_{g2l,k_m} = \text{diag}(\hat{\mathbf{h}}_{g2l,k_m}) \mathbf{X}_{g,k_m} \text{diag}(\hat{\mathbf{h}}_{g2l,k_m}^H), \quad (20c)$$

where $\mathbf{X}_{l,mn} = \mathbb{E}\{\Phi_{el,mn} \Phi_{el,mn}^H\}$, $\mathbf{X}_{l,mk_m} = \mathbb{E}\{\Phi_{el,mk_m} \Phi_{el,mk_m}^H\}$ and $\mathbf{X}_{g,k_m} = \mathbb{E}\{\Phi_{eg,k_m} \Phi_{eg,k_m}^H\}$. The symmetric residual channel matrixes are defined as $\tilde{\mathbf{H}}_{g,n} = \mathbb{E}\{\tilde{\mathbf{h}}_{g,n} \tilde{\mathbf{h}}_{g,n}^H\}$, $\tilde{\mathbf{H}}_{g2l,k_m} = \mathbb{E}\{\tilde{\mathbf{h}}_{g2l,k_m} \tilde{\mathbf{h}}_{g2l,k_m}^H\}$, $\tilde{\mathbf{H}}_{l,mk_m} = \mathbb{E}\{\tilde{\mathbf{h}}_{l,mk_m} \tilde{\mathbf{h}}_{l,mk_m}^H\}$. Based on the symmetric channel matrixes and beamforming matrixes, the power segments of the received signal can be reformulated as

$$S'_{g,cn} = \text{tr}(\mathbf{H}_{g,n} \mathbf{F}_{g,c}), \quad (21a)$$

$$\tilde{S}'_{g,cn} = \text{tr}(\tilde{\mathbf{H}}_{g,n} \mathbf{F}_{g,c}), \quad (21b)$$

$$S'_{g,dn} = \text{tr}(\mathbf{H}_{g,n} \mathbf{F}_{g,d}), \quad (21c)$$

$$\tilde{S}'_{g,dn} = \text{tr}(\tilde{\mathbf{H}}_{g,n} \mathbf{F}_{g,d}), \quad (21d)$$

$$S'_{g2l,ck_m} = \text{tr}(\mathbf{H}_{g2l,k_m} \mathbf{F}_{g,c}), \quad (21e)$$

$$\tilde{S}'_{g2l,ck_m} = \text{tr}(\tilde{\mathbf{H}}_{g2l,k_m} \mathbf{F}_{g,c}), \quad (21f)$$

$$S'_{l,ck_m} = \text{tr}(\mathbf{H}_{l,mk_m} \mathbf{F}_{l,cm}), \quad (21g)$$

$$\tilde{S}'_{l,ck_m} = \text{tr}(\tilde{\mathbf{H}}_{l,mk_m} \mathbf{F}_{l,cm}), \quad (21h)$$

$$S'_{l,pk_m} = \text{tr}(\mathbf{H}_{l,mk_m} \mathbf{F}_{l,pk_m}), \quad (21i)$$

$$\tilde{S}'_{l,pk_m} = \text{tr}(\tilde{\mathbf{H}}_{l,mk_m} \mathbf{F}_{l,pk_m}), \quad (21j)$$

$$I_{g,n}^{tot'} = \sum_{m=1}^M \text{tr}(\mathbf{H}_{l2g,mn} \mathbf{F}_{l,cm}) + \sum_{m=1}^M \sum_{i=1}^{K_m} \text{tr}(\mathbf{H}_{l2g,mn} \mathbf{F}_{l,pi}), \quad (21k)$$

$$I_{l,k_m}^{tot'} = \sum_{\substack{i=1, \\ i \neq k_m}}^{K_m} \text{tr}(\mathbf{H}_{l,mk_m} \mathbf{F}_{l,pi}) + \sum_{\substack{j=1, \\ j \neq m}}^M \text{tr}(\mathbf{H}_{l,jk_m} \mathbf{F}_{l,cj}) + \sum_{j=1}^M \sum_{\substack{i=1 \\ j \neq m}}^{K_j} \text{tr}(\mathbf{H}_{l,jk_m} \mathbf{F}_{l,pi}) + \text{tr}(\mathbf{H}_{g2l,k_m} \mathbf{F}_{g,d}). \quad (21l)$$

The ergodic rate is approximated by the following method as in [35], take the general rate expression as an example,

$$R = \mathbb{E}\{\log_2(1 + \frac{c_1}{c_2})\} \approx \log_2(1 + \frac{\mathbb{E}\{c_1\}}{\mathbb{E}\{c_2\}}), \quad (22)$$

where c_1 and c_2 are nonnegative random variable. Therefore,

the rate expressions can be redefined and approximated as

$$R'_{g,cn} \approx \log_2 \left(\frac{S'_{g,cn} + S'_{g,dn} + I_{g,n}^{tot'} + \sigma_n^2}{\tilde{S}'_{g,cn} + \tilde{S}'_{g,dn} + I_{g,n}^{tot'} + \sigma_n^2} \right) \quad (23a)$$

$$R'_{g,dn} \approx \log_2 \left(\frac{\tilde{S}'_{g,cn} + S'_{g,dn} + I_{g,n}^{tot'} + \sigma_n^2}{\tilde{S}'_{g,cn} + \tilde{S}'_{g,dn} + I_{g,n}^{tot'} + \sigma_n^2} \right) \quad (23b)$$

$$R_{l,k_m}^{sup'} \approx \log_2 \left(\frac{S'_{g2l,ck_m} + S'_{l,ck_m} + S'_{l,pk_m} + I_{l,k_m}^{tot'} + \sigma_{k_m}^2}{\tilde{S}'_{g2l,ck_m} + S'_{l,ck_m} + S'_{l,pk_m} + I_{l,k_m}^{tot'} + \sigma_{k_m}^2} \right) \quad (23c)$$

$$R_{l,k_m}^{sub'} \approx \log_2 \left(\frac{\tilde{S}'_{g2l,ck_m} + S'_{l,ck_m} + S'_{l,pk_m} + I_{l,k_m}^{tot'} + \sigma_{k_m}^2}{\tilde{S}'_{g2l,ck_m} + \tilde{S}'_{l,ck_m} + S'_{l,pk_m} + I_{l,k_m}^{tot'} + \sigma_{k_m}^2} \right) \quad (23d)$$

$$R'_{p,k_m} \approx \log_2 \left(\frac{\tilde{S}'_{g2l,ck_m} + \tilde{S}'_{l,pk_m} + S'_{l,pk_m} + I_{l,k_m}^{tot'} + \sigma_{k_m}^2}{\tilde{S}'_{g2l,ck_m} + \tilde{S}'_{l,ck_m} + \tilde{S}'_{l,pk_m} + I_{l,k_m}^{tot'} + \sigma_{k_m}^2} \right). \quad (23e)$$

In order to solve the non-convex parts in the rate expressions, we further introduce slack variables $\boldsymbol{\eta} = \{\eta_{g,c}, \eta_{g,p}, \boldsymbol{\eta}_l^{sup}, \boldsymbol{\eta}_l^{sub}, \boldsymbol{\eta}_p\}$ and $\boldsymbol{\xi} = \{\boldsymbol{\xi}_{g,c}, \boldsymbol{\xi}_{g,p}, \boldsymbol{\xi}_l^{sup}, \boldsymbol{\xi}_l^{sub}, \boldsymbol{\xi}_p\}$, where $\boldsymbol{\eta}_{g,c} \triangleq [\eta_{g,c1}, \dots, \eta_{g,cN}]^T$, $\boldsymbol{\eta}_{g,p} \triangleq [\eta_{g,p1}, \dots, \eta_{g,pN}]^T$, $\boldsymbol{\eta}_l^{sup} \triangleq [\eta_{l,1}^{sup}, \dots, \eta_{l,K}^{sup}]^T$, $\boldsymbol{\eta}_l^{sub} \triangleq [\eta_{l,1}^{sub}, \dots, \eta_{l,K}^{sub}]^T$, $\boldsymbol{\eta}_p \triangleq [\eta_{p,1}, \dots, \eta_{p,K}]^T$. $\boldsymbol{\xi}_{g,c} \triangleq [\xi_{g,c1}, \dots, \xi_{g,cN}]^T$, $\boldsymbol{\xi}_{g,p} \triangleq [\xi_{g,p1}, \dots, \xi_{g,pN}]^T$, $\boldsymbol{\xi}_l^{sup} \triangleq [\xi_{l,1}^{sup}, \dots, \xi_{l,K}^{sup}]^T$, $\boldsymbol{\xi}_l^{sub} \triangleq [\xi_{l,1}^{sub}, \dots, \xi_{l,K}^{sub}]^T$, $\boldsymbol{\xi}_p \triangleq [\xi_{p,1}, \dots, \xi_{p,K}]^T$. By taking GU-n's lower bound of private rate as an example, $\alpha_{g,dn} \leq R'_{g,dn}$, it can be transformed as

$$\alpha_{g,dn} \ln 2 \leq \ln \left(\frac{\tilde{S}'_{g,cn} + S'_{g,dn} + I_{g,n}^{tot'} + \sigma_n^2}{\tilde{S}'_{g,cn} + \tilde{S}'_{g,dn} + I_{g,n}^{tot'} + \sigma_n^2} \right) \quad (24a)$$

$$= \ln(\tilde{S}'_{g,cn} + S'_{g,dn} + I_{g,n}^{tot'} + \sigma_n^2) - \ln(\tilde{S}'_{g,cn} + \tilde{S}'_{g,dn} + I_{g,n}^{tot'} + \sigma_n^2) \quad (24b)$$

$$= \eta_{g,dn} - \xi_{g,dn}, \quad (24c)$$

where $\eta_{g,dn}$ and $\xi_{g,dn}$ represent the lower bound and upper bound of corresponding terms, respectively.

Based on the auxiliary variables, \mathcal{P}_2 can be rewritten as \mathcal{P}_3 .

$$f_P = \beta \left\{ \left[\text{tr}(\mathbf{F}_{g,c}) - \left(\mathbf{v}_{\max g,c}^{[i]} \right)^H \mathbf{F}_{g,c} \mathbf{v}_{\max g,c}^{[i]} \right] + \left[\text{tr}(\mathbf{F}_{g,d}) - \left(\mathbf{v}_{\max g,p}^{[i]} \right)^H \mathbf{F}_{g,d} \mathbf{v}_{\max g,p}^{[i]} \right] \right. \\ \left. + \sum_{m=1}^M \left[\text{tr}(\mathbf{F}_{l,cm}) - \left(\mathbf{v}_{\max l,cm}^{[i]} \right)^H \mathbf{F}_{l,cm} \mathbf{v}_{\max l,cm}^{[i]} \right] + \sum_{m=1}^M \sum_{k_m=1}^{K_m} \left[\text{tr}(\mathbf{F}_{l,pk_m}) - \left(\mathbf{v}_{\max l,pk_m}^{[i]} \right)^H \mathbf{F}_{l,pk_m} \mathbf{v}_{\max l,pk_m}^{[i]} \right] \right\}. \quad (26)$$

$$\mathcal{P}_3 : \quad \max_{\mathbf{F}, \alpha, \mathbf{c}} \quad t \quad (25a)$$

$$\text{s.t.} \quad \alpha_{g,cn} \ln 2 \leq \eta_{g,cn} - \xi_{g,cn}, \quad n \in \mathcal{N} \quad (25b)$$

$$S'_{g,cn} + S'_{g,dn} + I_{g,n}^{tot'} + \sigma_n^2 \geq e^{\eta_{g,cn}} \quad (25c)$$

$$\tilde{S}'_{g,cn} + S'_{g,dn} + I_{g,n}^{tot'} + \sigma_n^2 \leq e^{\xi_{g,cn}} \quad (25d)$$

$$\alpha_{g,dn} \ln 2 \leq \eta_{g,dn} - \xi_{g,dn}, \quad n \in \mathcal{N} \quad (25e)$$

$$\tilde{S}'_{g,cn} + S'_{g,dn} + I_{g,n}^{tot'} + \sigma_n^2 \geq e^{\eta_{g,dn}} \quad (25f)$$

$$\tilde{S}'_{g,cn} + \tilde{S}'_{g,dn} + I_{g,n}^{tot'} + \sigma_n^2 \leq e^{\xi_{g,dn}} \quad (25g)$$

$$\alpha_{l,k_m}^{sup} \ln 2 \leq \eta_{l,k_m}^{sup} - \xi_{l,k_m}^{sup}, \quad k_m \in \mathcal{K}_m, \quad m \in \mathcal{M} \quad (25h)$$

$$S'_{g2l,ck_m} + S'_{l,ck_m} + S'_{l,pk_m} + I_{l,k_m}^{tot'} + \sigma_{k_m}^2 \geq e^{\eta_{l,k_m}^{sup}} \quad (25i)$$

$$\tilde{S}'_{g2l,ck_m} + S'_{l,ck_m} + S'_{l,pk_m} + I_{l,k_m}^{tot'} + \sigma_{k_m}^2 \leq e^{\xi_{l,k_m}^{sup}} \quad (25j)$$

$$\alpha_{l,k_m}^{sub} \ln 2 \leq \eta_{l,k_m}^{sub} - \xi_{l,k_m}^{sub}, \quad k_m \in \mathcal{K}_m, \quad m \in \mathcal{M} \quad (25k)$$

$$\tilde{S}'_{g2l,ck_m} + S'_{l,ck_m} + S'_{l,pk_m} + I_{l,k_m}^{tot'} + \sigma_{k_m}^2 \geq e^{\eta_{l,k_m}^{sub}} \quad (25l)$$

$$\tilde{S}'_{g2l,ck_m} + \tilde{S}'_{l,ck_m} + S'_{l,pk_m} + I_{l,k_m}^{tot'} + \sigma_{k_m}^2 \leq e^{\xi_{l,k_m}^{sub}} \quad (25m)$$

$$\alpha_{p,k_m} \ln 2 \leq \eta_{p,k_m} - \xi_{p,k_m}, \quad k_m \in \mathcal{K}_m, \quad m \in \mathcal{M} \quad (25n)$$

$$\tilde{S}'_{g2l,ck_m} + \tilde{S}'_{l,ck_m} + S'_{l,pk_m} + I_{l,k_m}^{tot'} + \sigma_{k_m}^2 \geq e^{\eta_{p,k_m}} \quad (25o)$$

$$\tilde{S}'_{g2l,ck_m} + \tilde{S}'_{l,ck_m} + \tilde{S}'_{l,pk_m} + I_{l,k_m}^{tot'} + \sigma_{k_m}^2 \leq e^{\xi_{p,k_m}} \quad (25p)$$

$$(18b) - (18o).$$

Note that (25d), (25g), (25j), (25m) and (25p) are nonconvex with convex Right-Hand Side (RHS) which can be approximated by the first-order Taylor series. The RHS parts of the above constraints are approximated at $\left\{ \xi_{g,cn}^{[i]}, \xi_{g,dn}^{[i]}, \xi_{l,k_m}^{sup [i]}, \xi_{l,k_m}^{sub [i]}, \xi_{p,k_m}^{[i]} | n \in \mathcal{N}, k_m \in \mathcal{K}_m, m \in \mathcal{M} \right\}$ at iteration i as (27)

$$e^j \leq e^{j^{[i]}} [j - j^{[i]} + 1], \quad (27)$$

where $j \in \left\{ \xi_{g,cn}, \xi_{g,dn}, \xi_{l,k_m}^{sup}, \xi_{l,k_m}^{sub}, \xi_{p,k_m} \right\}$. Hence, the constraints (25d), (25g), (25j), (25m) and (25p) can be rewritten as

$$\tilde{S}'_{g,cn} + S'_{g,dn} + I_{g,n}^{tot'} + \sigma_n^2 \leq e^{\xi_{g,cn}^{[i]}} [\xi_{g,cn} - \xi_{g,cn}^{[i]} + 1] \quad (28a)$$

$$\tilde{S}'_{g,cn} + \tilde{S}'_{g,dn} + I_{g,n}^{tot'} + \sigma_n^2 \leq e^{\xi_{g,dn}^{[i]}} [\xi_{g,dn} - \xi_{g,dn}^{[i]} + 1] \quad (28b)$$

$$\tilde{S}'_{g2l,ck_m} + S'_{l,ck_m} + S'_{l,pk_m} + I_{l,k_m}^{tot'} + \sigma_{k_m}^2 \leq e^{\xi_{l,k_m}^{sup [i]}} [\xi_{l,k_m}^{sup} - \xi_{l,k_m}^{sup [i]} + 1] \quad (28c)$$

$$\tilde{S}'_{g2l,ck_m} + \tilde{S}'_{l,ck_m} + S'_{l,pk_m} + I_{l,k_m}^{tot'} + \sigma_{k_m}^2 \leq e^{\xi_{l,k_m}^{sub [i]}} [\xi_{l,k_m}^{sub} - \xi_{l,k_m}^{sub [i]} + 1] \quad (28d)$$

$$\tilde{S}'_{g2l,ck_m} + \tilde{S}'_{l,ck_m} + \tilde{S}'_{l,pk_m} + I_{l,k_m}^{tot'} + \sigma_{k_m}^2 \leq e^{\xi_{p,k_m}^{[i]}} [\xi_{p,k_m} - \xi_{p,k_m}^{[i]} + 1]. \quad (28e)$$

Rank-one implies that there is only one nonzero eigenvalue, hence, the nonconvex constraints (18l) and (18n) can be reexpressed as

$$\text{tr}(\mathbf{F}_{g,c}) - \lambda_{\max}(\mathbf{F}_{g,c}) = 0, \quad \text{tr}(\mathbf{F}_{g,d}) - \lambda_{\max}(\mathbf{F}_{g,d}) = 0, \quad (29a)$$

$$\text{tr}(\mathbf{F}_{l,cm}) - \lambda_{\max}(\mathbf{F}_{l,cm}) = 0, \quad m \in \mathcal{M}, \quad (29b)$$

$$\text{tr}(\mathbf{F}_{l,pk_m}) - \lambda_{\max}(\mathbf{F}_{l,pk_m}) = 0, \quad k_m \in \mathcal{K}_m, \quad m \in \mathcal{M}. \quad (29c)$$

In order to include these constraints into the objective function (25a), we construct a penalty function and obtain

$$\max_{\mathbf{F}, \alpha, \mathbf{c}} \quad t - \beta \left\{ [\text{tr}(\mathbf{F}_{g,c}) - \lambda_{\max}(\mathbf{F}_{g,c})] \right. \\ \left. + [\text{tr}(\mathbf{F}_{g,d}) - \lambda_{\max}(\mathbf{F}_{g,d})] \right. \\ \left. + \sum_{m=1}^M [\text{tr}(\mathbf{F}_{l,cm}) - \lambda_{\max}(\mathbf{F}_{l,cm})] \right. \\ \left. + \sum_{m=1}^M \sum_{k_m=1}^{K_m} [\text{tr}(\mathbf{F}_{l,pk_m}) - \lambda_{\max}(\mathbf{F}_{l,pk_m})] \right\}. \quad (30)$$

To ensure that the penalty function is as small as possible, we choose the appropriate penalty factor β . Due to the existence of the penalty function, (30) is not concave. We utilize an iterative approach to solve this problem [35]. Using $\text{tr}(\mathbf{F}_{g,c}) - \lambda_{\max}(\mathbf{F}_{g,c})$ as an example, the following inequality can be derived

$$0 \leq \text{tr}(\mathbf{F}_{g,c}) - \lambda_{\max}(\mathbf{F}_{g,c}) \\ \leq \text{tr}(\mathbf{F}_{g,c}) - \left(\mathbf{v}_{\max g,c}^{[i]} \right)^H \mathbf{F}_{g,c} \mathbf{v}_{\max g,c}^{[i]}, \quad (31)$$

Algorithm 1: SDP-based Optimization Scheme

```

1 Initialize:  $i \leftarrow 0$ ,  $t^{[i]} \leftarrow 0$ ,  $\mathbf{F}^{[i]}$ ,  $\boldsymbol{\xi}^{[i]}$ ;
2 repeat
3    $i \leftarrow i + 1$ ;
4   Solve problem (32) using  $\mathbf{F}^{[i-1]}$ ,  $\boldsymbol{\xi}^{[i-1]}$  and denote
   the optimal value of the objective function as
    $\{t - f_P\}^*$  and the optimal solutions as  $\mathbf{F}^*$ ,  $\boldsymbol{\xi}^*$ ;
5   Update  $\{t - f_P\}^{[i]} \leftarrow \{t - f_P\}^*$ ,  $\mathbf{F}^{[i]} \leftarrow \mathbf{F}^*$ ,
    $\boldsymbol{\xi}^{[i]} \leftarrow \boldsymbol{\xi}^*$ ;
6 until  $|\{t - f_P\}^{[i]} - \{t - f_P\}^{[i-1]}| < \tau$ ;
7 for  $j \in \{\{g, c\}, \{g, p\}, \{l, cm\}, \{l, pk\} | k \in \mathcal{K},$ 
    $m \in \mathcal{M}\}$  do
8   if  $\text{rank}(\mathbf{F}_j) = 1$  then
9     Use eigenvalue decomposition to  $\mathbf{F}_j$  and obtain
     the corresponding precoder
10  else
11    Use randomization to extract an approximate
    solution
12  end
13 end

```

where $\mathbf{v}_{\max g,c}$ is a normalized eigenvector in association with the largest eigenvalue $\lambda_{\max}(\mathbf{F}_{g,c})$. Likewise, we define $\mathbf{v}_{\max g,p}$ for $\lambda_{\max}(\mathbf{F}_{g,d})$ and $\mathbf{v}_{\max l,cm}$ for $\lambda_{\max}(\mathbf{F}_{l,cm})$ as well as $\mathbf{v}_{\max l,pk_m}$ for $\lambda_{\max}(\mathbf{F}_{l,pk_m})$'s associated eigenvectors. The iterative penalty function is represented by f_P in (26).

Therefore, we solve the following subproblem:

$$\begin{aligned}
\mathcal{P}_4 : \quad & \max_{\substack{\mathbf{F}, \boldsymbol{\alpha}, \mathbf{c} \\ \eta, \boldsymbol{\xi}}} & t - f_P & (32a) \\
\text{s.t.} \quad & & (18b) - (18k), (18o), (25b), \\
& & (25c), (25e), (25f), (25h), (25i), \\
& & (25k), (25l), (25n), (25o), (28).
\end{aligned}$$

Problem \mathcal{P}_1 has been transformed into convex problem and can be solved effectively using the CVX toolbox [36]. While solving \mathcal{P}_4 , the results $\{\mathbf{F}^{[i]}, \boldsymbol{\xi}^{[i]}\}$ from the i -th iteration are considered as constants. The existence of lower bounds, i.e., (31), ensures that the objective function converges. In other words, the rank-one constraints can be satisfied [35]. If the optimized symmetric matrices, $\{\mathbf{F}_{g,c}, \mathbf{F}_{g,p}, \mathbf{F}_{l,cm}, \mathbf{F}_{l,pk} | k \in \mathcal{K}, m \in \mathcal{M}\}$, are of rank one, then the optimal precoders of GEO and LEO satellites can be obtained by using eigenvalue decomposition. Alternatively, randomization can be adopted to extract approximate solutions from the optimized symmetric matrices, however, this leads to higher complexity.

The steps of multilayer D-RSMA joint GEO-LEO precoders optimization scheme is summarized in Algorithm 1. The precoders are initialized by using Maximum Ratio Transmission (MRT) and Singular Value Decomposition (SVD) since they have been demonstrated to provide good overall performance over a variety of channel realizations [10], [37]. The tolerance of the algorithm is denoted by $\tau = 10^{-5}$.

The convergence of Algorithm 1 is guaranteed since the solutions to the problem (32) at iteration $i - 1$ is a feasible

TABLE II
SIMULATION PARAMETERS

Parameter	GEO	LEO
Carrier frequency	20 GHz	
Bandwidth	500 MHz	
User terminal antenna gain	39.7 dBi	
Boltzmann constan	$1.38 \times 10^{-23} \text{ J} \cdot \text{K}^{-1}$	
Noise temperature	290 K	
Satellite height	35786 km	600 km
Antenna gain	58.5 dBi	30.5 dBi
3 dB bandwidth	0.4412 deg	4.4127 deg
Rician factor		10 dB

solution to the problem at iteration i . Therefore, the objective function $t - f_P$ rises monotonically and it is constrained above by the transmit power. At each iteration, the solution meets the Karush-Kuhn-Tucker (KKT) optimality criteria, which are the same as those of (17) at convergence [38]. The total number of iterations required for the convergence is approximated as $\mathcal{O}(\log(\tau^{-1}))$. At each iteration of the proposed SDP-based algorithm, the convex subproblem \mathcal{P}_4 is solved. The computational complexity of each iteration is mostly determined by the number of optimization variables, the number and size of Linear Matrix Inequality (LMI) constraints, and the size of Second Order Cone (SOC) constraints [39], [40]. The problem \mathcal{P}_4 has $2N_{tg}^2 + (K + M)N_{tl}^2 + 2K + N$ design variables, $6N + 9K + 1$ slack variables, and $8N + 12K + M + 1$ LMI constraints of size 1. Therefore, the worst-case computational complexity is given by

$$\begin{aligned}
& \mathcal{O}\left(\log(\tau^{-1})(8N + 12K + M + 1)^{1/2} \cdot z \left[z^2 \right. \right. \\
& \quad \left. \left. + 2N_{tg}^2(N_{tg} + z) + (K + M)N_{tl}^2(N_{tl} + z) \right. \right. \\
& \quad \left. \left. + (2K + N)(1 + z) + (8N + 12K + M + 1)(1 + z) \right] \right), & (33)
\end{aligned}$$

where $z = \mathcal{O}(2N_{tg}^2 + (K + M)N_{tl}^2 + 2K + N + 6N + 9K)$.

IV. SIMULATION RESULTS

The performance of the proposed D-RSMA scheme is evaluated in this section. We assume all GEO and LEO satellites operate in the Ka-band [2], [3], [22]. The major simulation parameters are listed in Table II. Specifically, we assume the GEO satellite is equipped with $N_{tg} = 4$ antennas, and $N = 6$ multicasting GUs locate uniformly in coverage area. Each LEO satellite is deployed with $N_{tl} = 3$ antennas, and LUs are uniformly distributed within LEO coverage. Because the noise power is normalized by $\kappa T_{sys} B_w$ in (4) and (7), we denote unit noise variance, i.e., $\sigma_r^2 = \sigma_n^2 = \sigma_{k_m}^2 = 1$, $\forall n \in \mathcal{N}$, $\forall k_m \in \mathcal{K}$, $m \in \mathcal{M}$. We redefine P_l as Signal-to-Noise Ratio (SNR) of LEO satellite and P_g as SNR of GEO satellite. We first investigate the scenario with perfect CSI in the network, then we move to the deployment with imperfect CSIT and

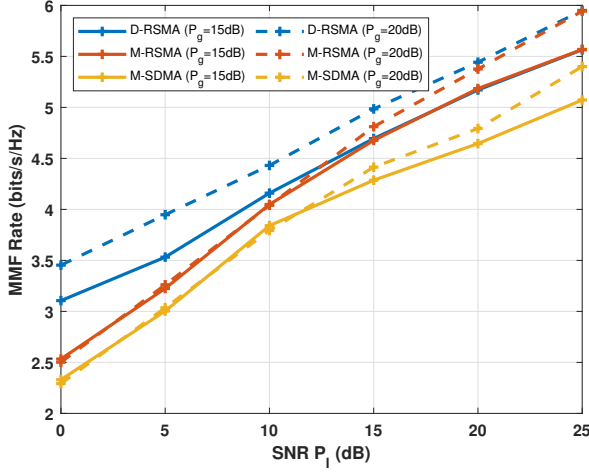


Fig. 3. MMF rate versus LEO SNR P_l for different GEO SNR P_g and network loads. $N_{tg} = 4$, $N_{tl} = 3$, $M = 2$, $N = 6$, $K = 4$.

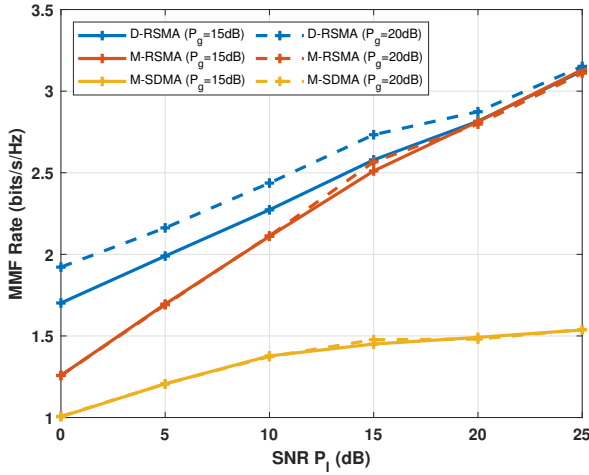


Fig. 4. MMF rate versus LEO SNR P_l for different GEO SNR P_g and network loads. $N_{tg} = 4$, $N_{tl} = 3$, $M = 2$, $N = 6$, $K = 8$.

imperfect CSIR. All MMF simulation results are obtained by averaging 100 channel realizations.

We compare the D-RSMA with two baseline multiple access schemes, namely, “M-RSMA” and “M-SDMA”. “M-RSMA” means multicasting is adopted at the GEO satellite and LEO satellites adopt 1-layer RSMA, while “M-SDMA” denotes multicasting is adopted at the GEO and LEO satellites implement SDMA.

Fig. 3 and 4 compare the MMF performance of D-RSMA and baseline schemes under different system setups. Fig. 3 shows the MMF performance under 2 LEO satellites and 4 LUs deployments, each LEO satellite serves 2 LUs. Fig. 4 illustrates the MMF rate for overloaded scenario, i.e., 8 LUs in total, and 4 LUs are served by one LEO satellite. From both figures, it can be seen that D-RSMA achieves a clear MMF rate gain over all the other schemes. As P_l increases, the gap between D-RSMA and M-RSMA schemes gradually decreases and the two schemes overlap when P_l is large enough. The reasons are as follows. The joint GEO-LEO beamforming

optimization method is designed to attain the optimized MMF rates. When the power budget of LEO is relatively small, the system performance is restricted by the LUs since the SINRs of LUs are much lower than those of GUs. However, in the D-RSMA scheme, LUs messages are divided and parts of LUs’ data are encoded into common stream $s_{g,c}$ transmitted from the GEO satellite (streams are transmitted from different satellites, thereby RSMA is distributedly implemented). This enables D-RSMA to utilize GEO power to transmit parts of LUs data, balancing the network load and managing the interference between two sub-networks. Due to the fixed GEO satellite transmit power budget P_g , the MMF rates of both D-RSMA and M-RSMA saturate when P_l is sufficiently large. The benefit of the D-RSMA over the other strategies decreases as P_l increases. M-RSMA outperforms M-SDMA because we consider the LoS channels and the LUs channels are closely aligned with each other. Compared to Fig. 3, the attained MMF rate in Fig. 4 decreases, while the benefit of distributed RSMA is enhanced further. The relative gain of “D-RSMA ($P_g = 15$ dB)” over “M-RSMA ($P_g = 15$ dB)” increases from 2.74% in Fig. 3 to 7.71% in Fig. 4 when $P_l = 10$ dB. With more served LUs, the simultaneous inter-system and intra-system interference are severer. M-RSMA cannot manage the interference between sub-networks. However, by transmitting $s_{g,c}$ from GEO, the interference can be coordinated and suppressed with the implementation of D-RSMA.

The influence of the GEO power budget is also investigated. From Fig. 3, the larger P_g leads to better MMF rate performance. Besides, D-RSMA benefits more from the increase in power budget since GEO can allocate more power to transmit the common message. Hence the overall max-min rate can be improved and the saturated rate when P_l is sufficiently large increases compared to that in the scenario with $P_g = 15$ dB. When LEO satellites work in the overloaded deployment (Fig. 4), only D-RSMA benefits from the increase of P_g since it can make use of the power from both sub-networks and manage the severer interference between GEO and LEO sub-networks. We can conclude that D-RSMA can well manage the interference and achieves MMF rate gain compared to M-RSMA and M-SDMA regardless of network loads, which guarantees user fairness. Alternatively, D-RSMA can utilize less power to achieve the same MMF performance.

The influence of the number of LEO satellites is illustrated in Fig. 5. We illustrate the performance of proposed scheme in dense LEO networks with $M = 2$, $M = 4$ and $M = 8$ LEO satellites scenarios. 2 LUs are served by each LEO satellite. By increasing the number of LEO satellites and LUs, the MMF performances of all schemes degrade, while D-RSMA still outperforms the other baseline approaches in all deployments. The relative gain of D-RSMA over M-RSMA increases from 9.68% in 2 LEO satellites deployment to 13.74% in 4 LEO satellites and to 37.41% in 8 LEO satellites deployment when $P_l = 10$ dB. Because, as the increase of LEO satellites and LUs, each UT suffers from severer inter-system and intra-system interference, without the transmission of $s_{g,c}$, M-RSMA cannot manage the interference coming from GUs and LUs that are not served by the same LEO. In comparison, D-RSMA is more robust to the number of co-existence LEO

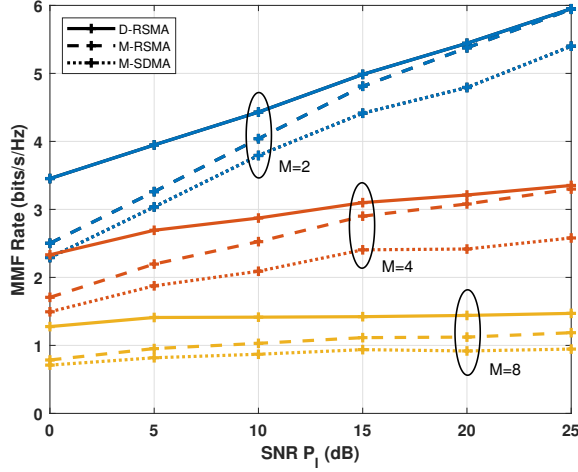


Fig. 5. MMF rate versus LEO SNR P_l with varied number of LEO satellites. $N_{tg} = 4$, $N_{tl} = 3$, $N = 6$, $P_g = 20$ dB.

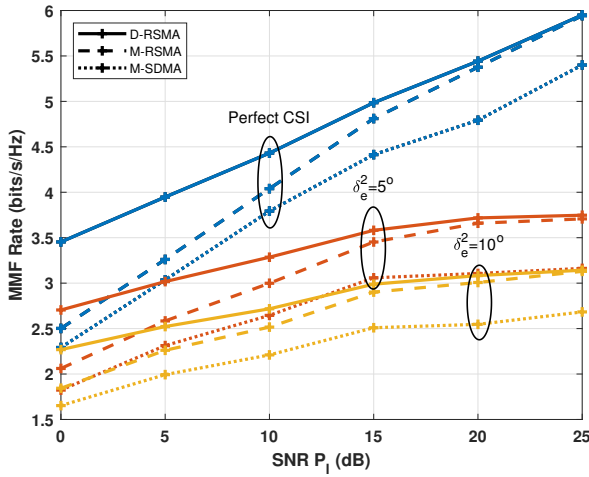


Fig. 6. MMF rate versus LEO SNR P_l with varied satellite phase uncertainties. $M = 2$, $N_{tg} = 4$, $N_{tl} = 3$, $N = 6$, $K = 4$, $P_g = 20$ dB.

satellites and network load thanks to its ability to partially decode the interference and partially treat interference as noise.

Furthermore, we take phase uncertainty into account. We assume $\sigma_{e,g}^2 = \sigma_{e,l}^2 = \sigma_e^2$. The ergodic MMF performance of the proposed method and baselines under imperfect CSIT and imperfect CSIR is investigated in Fig. 6. The MMF rates in all approaches decrease with a rise in phase uncertainty variation, while D-RSMA outperforms baselines in all scenarios. When $P_l = 20$ dB, from perfect CSI (i.e., $\sigma_e^2 = 0^\circ$) to the deployment with $\sigma_e^2 = 5^\circ$ and $\sigma_e^2 = 10^\circ$, the corresponding ergodic MMF rate decreases by 30.69% and 42.35% respectively for D-RSMA, and decreases by 32.93% and 45.06% respectively for M-SDMA. For comparison, the ergodic MMF rate of M-SDMA decreases by 36.19% and 47.86% from perfect CSI to the deployment with $\sigma_e^2 = 5^\circ$ and $\sigma_e^2 = 10^\circ$, respectively. D-RSMA and M-RSMA have a more flexible design that allows them to partially decode interference and treat it as noise. Therefore D-RSMA is more robust to channel phase uncertainty.

V. CONCLUSION

To conclude, we have investigated the co-existence of GEO-LEO multilayer network with statistical CSIT and CSIR, where the RSMA is distributedly implemented (D-RSMA) to mitigate the interference and improve user fairness. To this end, we have formulated a MMF problem that jointly optimizes the precoders of GEO and LEO satellites and the message split of each user subject to the power constraints at the satellites. We have proposed a robust SDP-based iterative optimization algorithm to solve this problem. We have further showed show through numerical results that the proposed D-RSMA can well manage the interference and boost the MMF performance of the system. The influence of the GEO power budget, the number of LUs, the number of LEO satellites and CSI uncertainty have been studied. We have found that D-RSMA is robust to the channel phase uncertainty. Besides, as the increase of GEO transmit power, or the number of serving LUs, the rate improvement of D-RSMA over other RSMA and SDMA baselines become more significant. Thanks to the transmission of GEO common stream, D-RSMA is more capable of managing inter-system and intra-system interference. These results lead us to conclude that D-RSMA is superior to existing transmission schemes and has a great potential to improve the system performance of future communication networks.

REFERENCES

- [1] 3GPP TR 22.822 V16.0.0, "3rd Generation Partnership Project; Technical Specification Group Services and System Aspects; Study on using Satellite Access in 5G; Stage 1 (Release 16)," 3GPP, techreport, Jun. 2018.
- [2] 3GPP TR 38.821 V16.1.0, "3rd Generation Partnership Project; Technical Specification Group Radio Access Network; Solutions for NR to support non-terrestrial networks (NTN) (Release 16)," 3GPP, techreport, May 2021.
- [3] 3GPP TR 38.811 V15.4.0, "3rd Generation Partnership Project; Technical Specification Group Radio Access Network; Study on New Radio (NR) to support non-terrestrial networks (Release 15)," 3GPP, techreport, Sep. 2020.
- [4] Y. Liu, Y. Wang, J. Wang, L. You, W. Wang, and X. Gao, "Robust downlink precoding for LEO satellite systems with per-antenna power constraints," *IEEE Transactions on Vehicular Technology*, vol. 71, no. 10, pp. 10 694–10 711, Oct. 2022.
- [5] R. Li, P. Gu, and C. Hua, "Optimal beam power control for co-existing multibeam GEO and LEO satellite system," in *2019 11th International Conference on Wireless Communications and Signal Processing (WCSP)*, Oct. 2019, pp. 1–6.
- [6] P. Gu, R. Li, C. Hua, and R. Tafazolli, "Dynamic cooperative spectrum sharing in a multi-beam LEO-GEO co-existing satellite system," *IEEE Transactions on Wireless Communications*, vol. 21, no. 2, pp. 1170–1182, Feb. 2022.
- [7] C. Wang, D. Bian, S. Shi, J. Xu, and G. Zhang, "A novel cognitive satellite network with GEO and LEO broadband systems in the downlink case," *IEEE Access*, vol. 6, pp. 25 987–26 000, 2018.
- [8] J. Park, B. Lee, J. Choi, H. Lee, N. Lee, S.-H. Park, K.-J. Lee, J. Choi, S. H. Chae, S.-W. Jeon, K. S. Kwak, B. Clerckx, and W. Shin, "Rate-splitting multiple access for 6g networks: Ten promising scenarios and applications," *IEEE Network*, pp. 1–1, 2023.
- [9] H. Joudeh and B. Clerckx, "Robust transmission in downlink multiuser MISO systems: A rate-splitting approach," *IEEE Trans. Signal Processing*, vol. 64, no. 23, pp. 6227–6242, Dec. 2016.
- [10] Y. Mao, B. Clerckx, and V. O. Li, "Rate-splitting multiple access for downlink communication systems: Bridging, generalizing, and outperforming SDMA and NOMA," *Journal on Wireless Communications and Networking*, no. 133 (2018), 2018.
- [11] Y. Mao, O. Dizdar, B. Clerckx, R. Schober, P. Popovski, and H. V. Poor, "Rate-splitting multiple access: Fundamentals, survey, and future research trends," *IEEE Communications Surveys and Tutorials*, vol. 24, no. 4, pp. 2073–2126, Fourthquarter 2022.

- [12] A. Zappone, B. Matthiesen, and E. A. Jorswieck, "Energy efficiency in MIMO underlay and overlay device-to-device communications and cognitive radio systems," *IEEE Transactions on Signal Processing*, vol. 65, no. 4, pp. 1026–1041, Feb. 2017.
- [13] Y. Mao, B. Clerckx, and V. O. Li, "Energy efficiency of rate-splitting multiple access, and performance benefits over SDMA and NOMA," in *2018 15th International Symposium on Wireless Communication Systems (ISWCS)*, 2018, pp. 1–5.
- [14] Y. Mao, B. Clerckx, J. Zhang, V. O. K. Li, and M. A. Arafah, "Max-min fairness of K-user cooperative rate-splitting in MISO broadcast channel with user relaying," *IEEE Transactions on Wireless Communications*, vol. 19, no. 10, pp. 6362–6376, 2020.
- [15] Y. Xu, Y. Mao, O. Dizdar, and B. Clerckx, "Max-min fairness of rate-splitting multiple access with finite blocklength communications," *IEEE Transactions on Vehicular Technology*, vol. 72, no. 5, pp. 6816–6821, May 2023.
- [16] J. Xu, O. Dizdar, and B. Clerckx, "Rate-splitting multiple access for short-packet uplink communications: A finite blocklength analysis," *IEEE Communications Letters*, vol. 27, no. 2, pp. 517–521, Feb. 2023.
- [17] O. Dizdar, Y. Mao, Y. Xu, P. Zhu, and B. Clerckx, "Rate-splitting multiple access for enhanced URLLC and eMBB in 6G: Invited paper," in *2021 17th International Symposium on Wireless Communication Systems (ISWCS)*, 2021, pp. 1–6.
- [18] Y. Liu, B. Clerckx, and P. Popovski, "Network slicing for eMBB, URLLC, and mMTC: An uplink rate-splitting multiple access approach," 2022. [Online]. Available: <https://arxiv.org/pdf/2208.10841.pdf>
- [19] Y. Xu, Y. Mao, O. Dizdar, and B. Clerckx, "Rate-splitting multiple access with finite blocklength for short-packet and low-latency downlink communications," *IEEE Transactions on Vehicular Technology*, vol. 71, no. 11, pp. 12 333–12 337, Nov. 2022.
- [20] H. Joudeh and B. Clerckx, "Rate-splitting for max-min fair multigroup multicast beamforming in overloaded systems," *IEEE Transactions on Wireless Communications*, vol. 16, no. 11, pp. 7276–7289, Nov. 2017.
- [21] M. Caus, A. Pastore, M. Navarro, T. Ramirez, C. Mosquera, N. Noels, N. Alagha, and A. I. Perez-Neira, "Exploratory analysis of superposition coding and rate splitting for multibeam satellite systems," in *2018 15th International Symposium on Wireless Communication Systems (ISWCS)*, Aug 2018, pp. 1–5.
- [22] L. Yin and B. Clerckx, "Rate-splitting multiple access for multigroup multicast and multibeam satellite systems," *IEEE Transactions on Communications*, vol. 69, no. 2, pp. 976–990, Feb. 2021.
- [23] —, "Rate-splitting multiple access for satellite-terrestrial integrated networks: Benefits of coordination and cooperation," *IEEE Transactions on Wireless Communications*, vol. 22, no. 1, pp. 317–332, Jan. 2023.
- [24] J. Lee, J. Lee, L. Yin, W. Shin, and B. Clerckx, "Coordinated rate-splitting multiple access for integrated satellite-terrestrial networks with super-common message," *IEEE Transactions on Vehicular Technology*, pp. 1–6, 2023.
- [25] W. U. Khan, Z. Ali, E. Lagunas, A. Mahmood, M. Asif, A. Ihsan, S. Chatzinotas, B. Ottersten, and O. A. Dobre, "Rate splitting multiple access for next generation cognitive radio enabled LEO satellite networks," *IEEE Transactions on Wireless Communications*, pp. 1–1, 2023.
- [26] V. Jorroughi, M. A. Vazquez, and A. I. Prez-Neira, "Generalized multicast multibeam precoding for satellite communications," *IEEE Transactions on Wireless Communications*, vol. 16, no. 2, pp. 952–966, Feb. 2017.
- [27] G. Zheng, S. Chatzinotas, and B. Ottersten, "Generic optimization of linear precoding in multibeam satellite systems," *IEEE Transactions on Wireless Communications*, vol. 11, no. 6, pp. 2308–2320, Jun. 2012.
- [28] K.-X. Li, L. You, J. Wang, X. Gao, C. G. Tsinos, S. Chatzinotas, and B. Ottersten, "Downlink transmit design for massive MIMO LEO satellite communications," *IEEE Transactions on Communications*, vol. 70, no. 2, pp. 1014–1028, Feb. 2022.
- [29] L. You, K.-X. Li, J. Wang, X. Gao, X.-G. Xia, and B. Ottersten, "Massive MIMO transmission for LEO satellite communications," *IEEE Journal on Selected Areas in Communications*, vol. 38, no. 8, pp. 1851–1865, Aug. 2020.
- [30] F. Fontan, M. Vazquez-Castro, C. Cabado, J. Garcia, and E. Kubista, "Statistical modeling of the LMS channel," *IEEE Transactions on Vehicular Technology*, vol. 50, no. 6, pp. 1549–1567, Nov. 2001.
- [31] A. V. Bagrov, V. A. Leonov, A. S. Mitkin, A. F. Nasyrov, A. D. Ponomarenko, K. M. Pichkhadze, and V. K. Sysoev, "Single-satellite global positioning system," *Acta Astronautica*, vol. 117, pp. 332–337, 2015. [Online]. Available: <https://www.sciencedirect.com/science/article/pii/S0094576515003343>
- [32] L. You, X. Qiang, C. G. Tsinos, F. Liu, W. Wang, X. Gao, and B. Ottersten, "Beam squint-aware integrated sensing and communications for hybrid massive MIMO LEO satellite systems," *IEEE Journal on Selected Areas in Communications*, vol. 40, no. 10, pp. 2994–3009, Oct. 2022.
- [33] L. You, K.-X. Li, J. Wang, X. Gao, X.-G. Xia, and B. Ottersten, "LEO satellite communications with massive MIMO," in *ICC 2020 - 2020 IEEE International Conference on Communications (ICC)*, Jun. 2020, pp. 1–6.
- [34] J. An, O. Dizdar, B. Clerckx, and W. Shin, "Rate-splitting multiple access for multi-antenna broadcast channel with imperfect CSIT and CSIR," in *IEEE International Symposium on Personal, Indoor and Mobile Radio Communications (PIMRC)*, 2020.
- [35] J. Chu, X. Chen, C. Zhong, and Z. Zhang, "Robust design for NOMA-based multibeam LEO satellite internet of things," *IEEE Internet of Things Journal*, vol. 8, no. 3, pp. 1959–1970, Feb. 2021.
- [36] M. Grant, S. Boyd, and Y. Ye, "CVX: Matlab software for disciplined convex programming," 2008.
- [37] H. Joudeh and B. Clerckx, "Sum-rate maximization for linearly precoded downlink multiuser MISO systems with partial CSIT: A rate-splitting approach," *IEEE Transactions on Communications*, vol. 64, no. 11, pp. 4847–4861, Nov. 2016.
- [38] B. R. Marks and G. P. Wright, "A general inner approximation algorithm for nonconvex mathematical programs," *Operations Research*, vol. 26, no. 4, pp. 681–683, 1978. [Online]. Available: <http://www.jstor.org/stable/169728>
- [39] G. Zhou, C. Pan, H. Ren, K. Wang, and A. Nallanathan, "A framework of robust transmission design for IRS-aided MISO communications with imperfect cascaded channels," *IEEE Transactions on Signal Processing*, vol. 68, pp. 5092–5106, 2020.
- [40] A. Ben-Tal and A. Nemirovski, *Lectures on modern convex optimization: analysis, algorithms, and engineering applications*. SIAM, 2001.